2 *Bainitic Ferrite*

The growth of pearlite occurs at a common transformation front with the austenite. The growth of the ferrite and cementite phases is coupled and their compositions are complementary since the carbon which cannot be accommodated by the ferrite is incorporated into the cementite. This contrasts with bainite which occurs in separable stages, first the growth of ferrite, followed by the precipitation of carbides. This chapter deals with the ferritic component of bainite, focusing on its morphology, crystallography, constitution and kinetics.

2.1 Sheaves of Bainite

2.1.1 Morphology

Both upper and lower bainite consist of aggregates of plates of ferrite, separated by untransformed austenite, martensite or cementite (Fig. 2.1). The aggregates of plates are called *sheaves* (Aaronson and Wells, 1956) and the plates within each sheaf are the *sub-units*. The sub-units are not isolated from each other but are connected in three dimensions. It follows that they share a common crystallographic orientation.

Many observations, including two-surface analysis experiments, show that the shape of a sheaf is that of a wedge-shaped plate (Oblak *et al.*, 1964; Srinivasan and Wayman, 1968b). The thicker end of the wedge begins at the nucleation site which is usually an austenite grain surface. The sub-units which make up the sheaf have a lenticular plate or lath morphology, whose form is most prominent near the edge or tip of a sheaf where impingement effects are minimal (Fig. 2.2).

The shape is best observed in partly transformed specimens. The dimensions of a sub-unit are uniform within a sheaf because each sub-unit grows to a limiting size. New sub-units are most frequently nucleated near the tips of existing sub-units rather than on their sides. The overall morphology of a sheaf is illustrated in Fig. 2.3.

When the sub-units are in the form of laths, they are longest along the close-packed direction of the ferrite which is most parallel to a corresponding close-packed direction of the austenite (Davenport, 1974). As with martensite, plates tend to form at low temperatures, large carbon concentrations or in strong

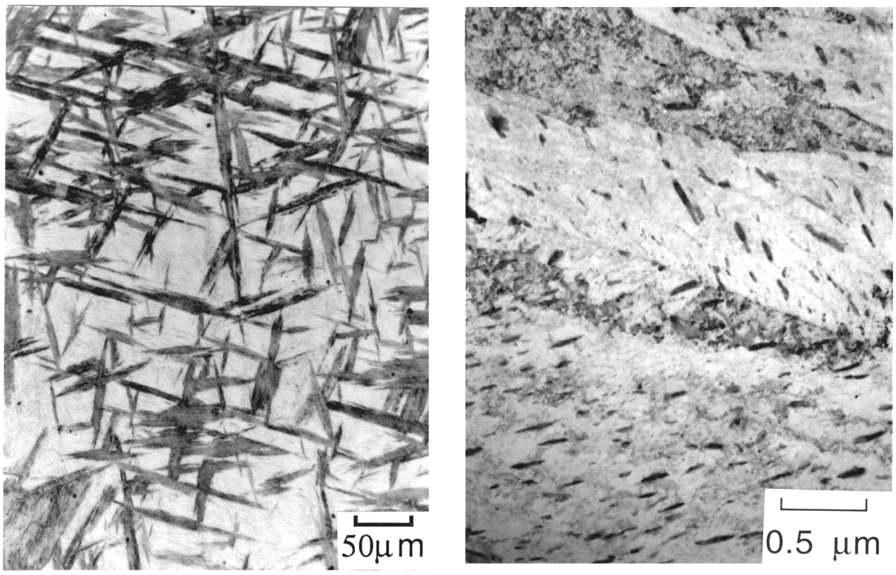

Fig. 2.1 (a) Light micrograph illustrating sheaves of lower bainite in a partially transformed (395 °C) Fe–0.3C–4Cr wt% alloy. The light etching matrix phase is martensite. (b) Corresponding transmission electron micrograph illustrating subunits of lower bainite.

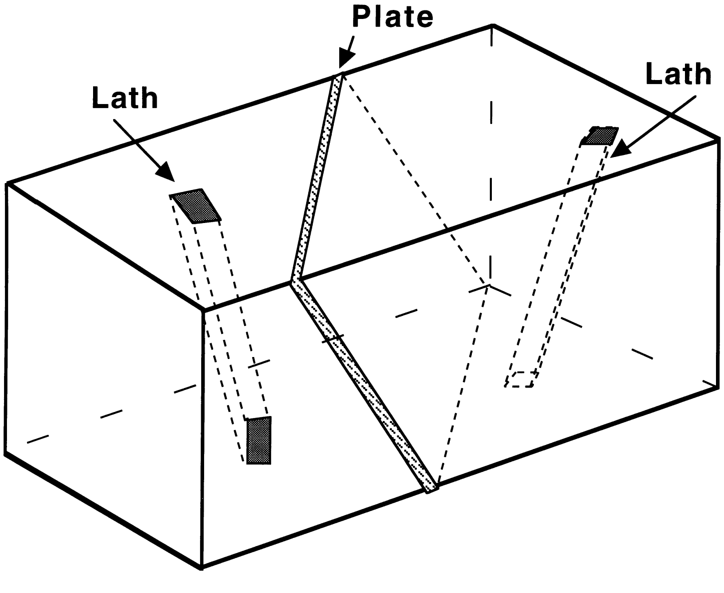

Fig. 2.2 The three-dimensional shape of a plate and of a lath.

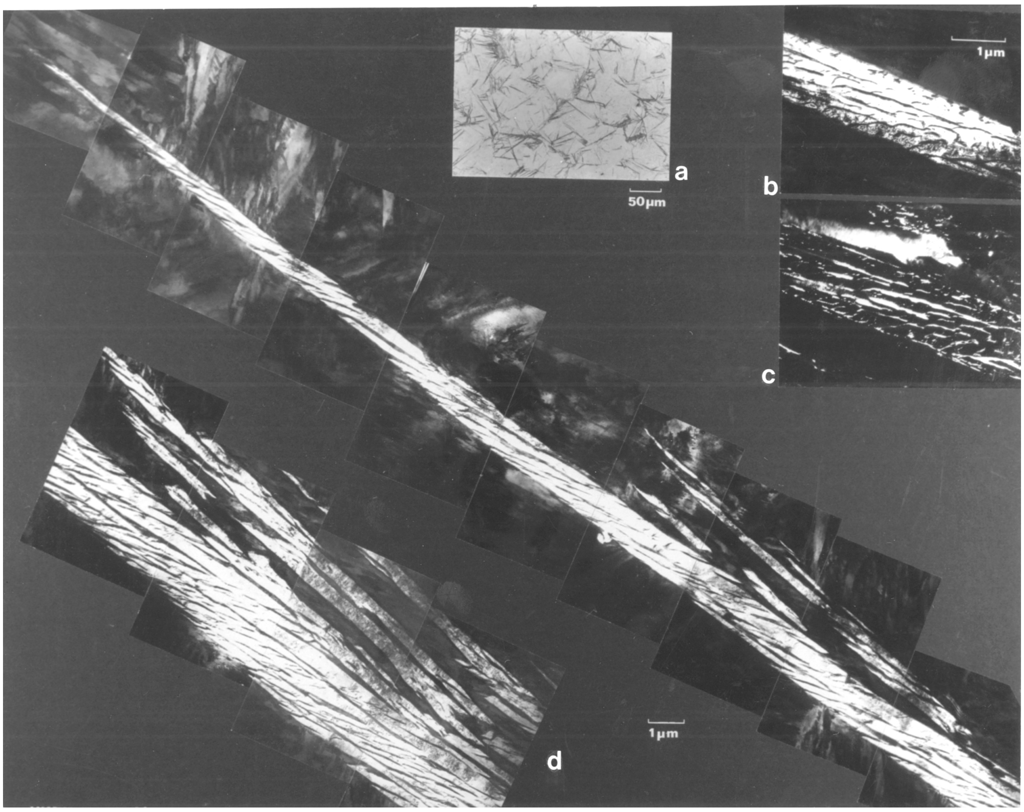

Fig. 2.3 Transmission electron micrograph of a sheaf of upper bainite in a partially transformed Fe–0.43C–2Si–3Mn wt% alloy: (a) light micrograph; (b, c) bright field and corresponding dark-field image of retained austenite between the sub-units; (d) montage showing the structure of the sheaf.

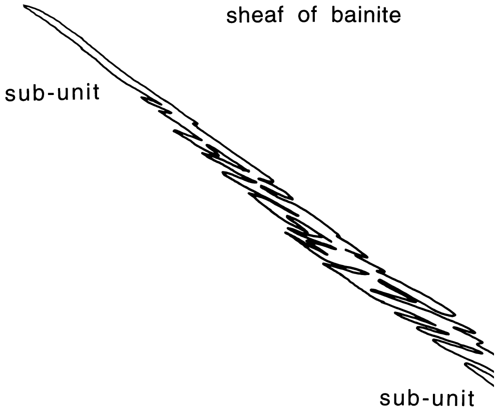

Fig. 2.3e Corresponding outline of the sub-units near the sheaf tip region.

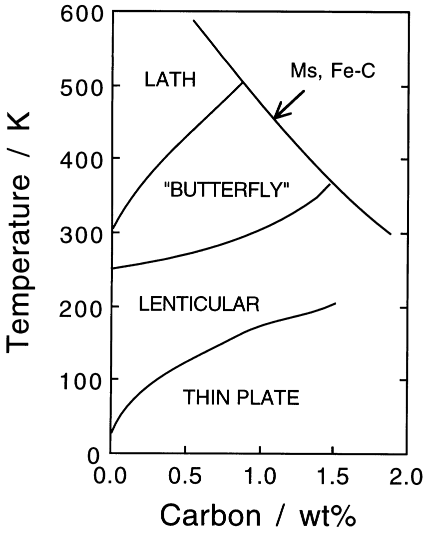

Fig. 2.4 The shape of martensite crystals as a function of the transformation temperature and carbon concentration of Fe–Ni–C alloys (after Maki and Tamura, 1986).

austenite, Fig. 2.4 (Kelly and Nutting, 1960; Davies and Magee, 1970a,b, 1971; Haezebrouck, 1987). Thus, a plate morphology can be induced by increasing the strength of the austenite even if the transformation temperature is increased at the same time (Laverrouz and Pineau, 1974). Similarly, the lath to plate transition can be induced using a magnetic field changing the driving force for transformation, without altering the transformation temperature (Korenko, 1973).

The physical basis for these correlations is not clear because the variables described are not independent. The strength of the austenite must play a role because it determines the extent to which the shape change is plastically accommodated. Lath martensite is associated with this plastic accommodation which ultimately stifles the growth of the lath.

This hypothesis has been developed in detail by Haezebrouck (1987) who proposed that a plate shape is promoted by rapid radial growth and a high yield stress in the parent phase. Both of these factors favour elastic growth. A high growth rate is equivalent to a high strain rate, which makes yielding more difficult. The radial growth must be elastic for small particles but whether this can be sustained as the particle grows depends on the flow behaviour of the austenite. The effect of plasticity is to cause the radial growth to arrest. If plasticity sets in at an early stage of growth, it is assumed that lath martensite is obtained. The model is consistent with experimental data, including the

Korenko experiment and the growth arrest. It does not, however, address the *shape* transition. A plate to lath transition depends on a change from isotropic to anisotropic radial growth.

The observed variations in microstructure as a function of temperature are summarised in Fig. 2.5.

Such changes in microstructure are illustrated vividly in Fig. 2.6, where the microstructure represents the effects of an abrupt change in the transformation temperature from 420°C to 290°C. This has resulted in a bimodal scale with a dramatic reduction in the plate size on lowering the temperature (Fig. 2.6).

2.1.2 *Thickness of bainite plates*

If the shape deformation is elastically accommodated then the plates can in principle maintain an elastic equilibrium with the matrix. They may continue to thicken isothermally until the strain energy balances the available free energy. It follows that if the plates are allowed to grow freely, they should be thicker at lower temperatures where the driving force is the greatest. This contradicts the experimental data because bainite is never elastically accommodated. Direct observations have shown that there is considerable plastic relaxation in the austenite adjacent to the bainite plates (Swallow and Bhadeshia, 1996). The dislocation debris generated in this process resists the

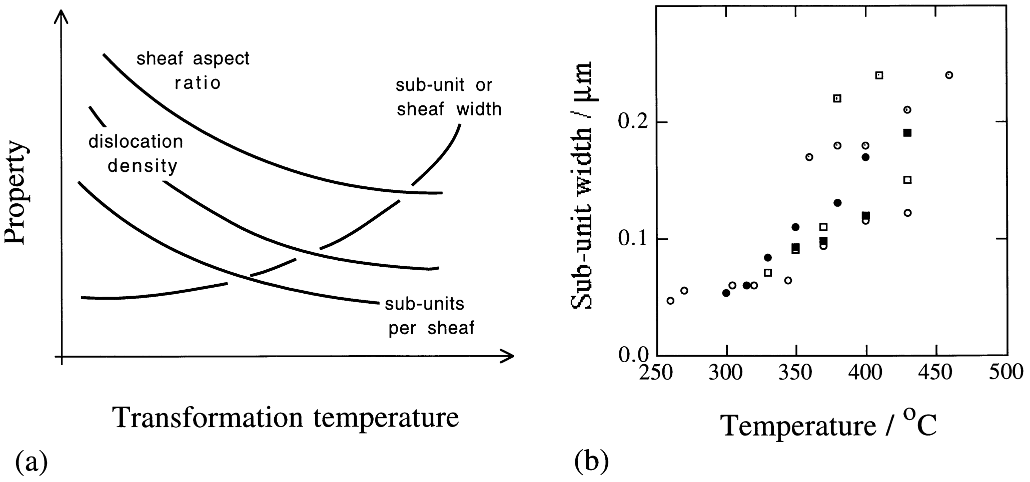

Fig. 2.5 (a) Qualitative trends in microstructure as a function of the transformation temperature. (b) Measurements of the bainite sub-unit thickness as a function of the transformation temperature for a variety of steels (Chang and Bhadeshia, 1995a; Singh and Bhadeshia, 1998.)

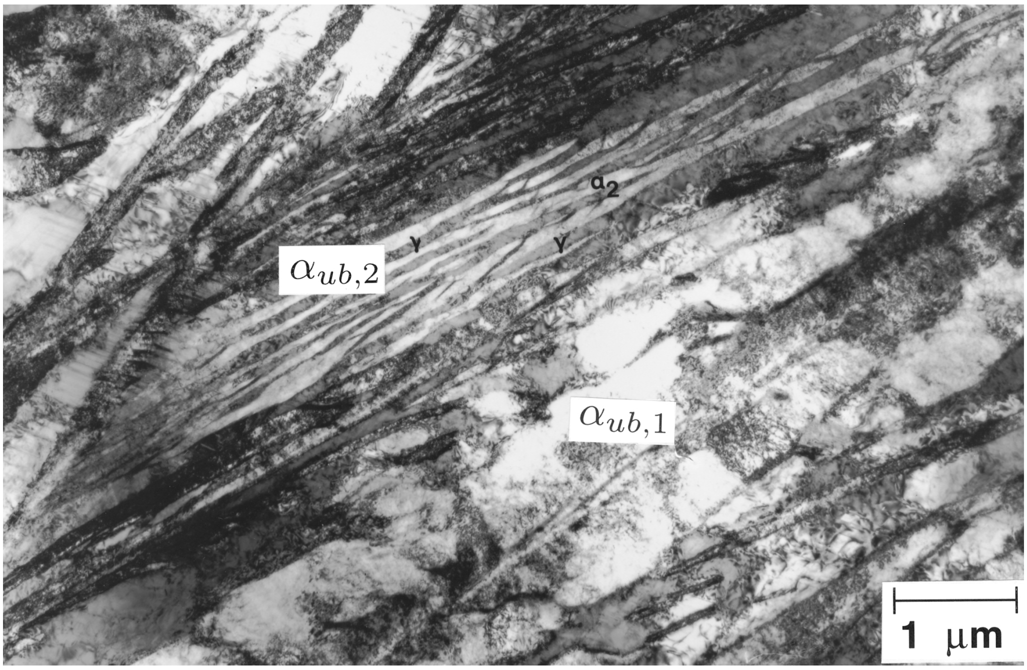

Fig. 2.6 A bimodal distribution of bainite plate thickness ($\alpha_{ub,1}$ and $\alpha_{ub,2}$, obtained by changing the isothermal transformation temperature from 420 °C to 290 °C. After Papadimitriou and Fourlaris (1997).

advance of the bainite/austenite interface, the resistance being greatest for strong austenite. The yield strength of the austenite must then feature in any assessment of plate size. In this scenario, the plates are expected to become thicker at high temperatures because the yield strength of the austenite will then be lower. Dynamic recovery at high temperatures may further weaken the austenite and lead to coarser plates. Indeed, high-temperature bainite often contains sub-grains which are finer for lower transformation temperatures (Pickering, 1958). These boundaries form by the recovery of the dislocation structure during transformation.

The thickness must also be influenced by impingement between adjacent plates; as in all transformations, a large nucleation rate corresponds to a finer microstructure.

The perceived effect of temperature could be indirect since both strength and the nucleation rate are strongly dependent on temperature. A quantitative analysis shows that temperature has only a small independent effect on the thickness of bainite plates (Fig. 2.7). The main conclusion is that strong austenite and high driving forces lead to a finer microstructure.

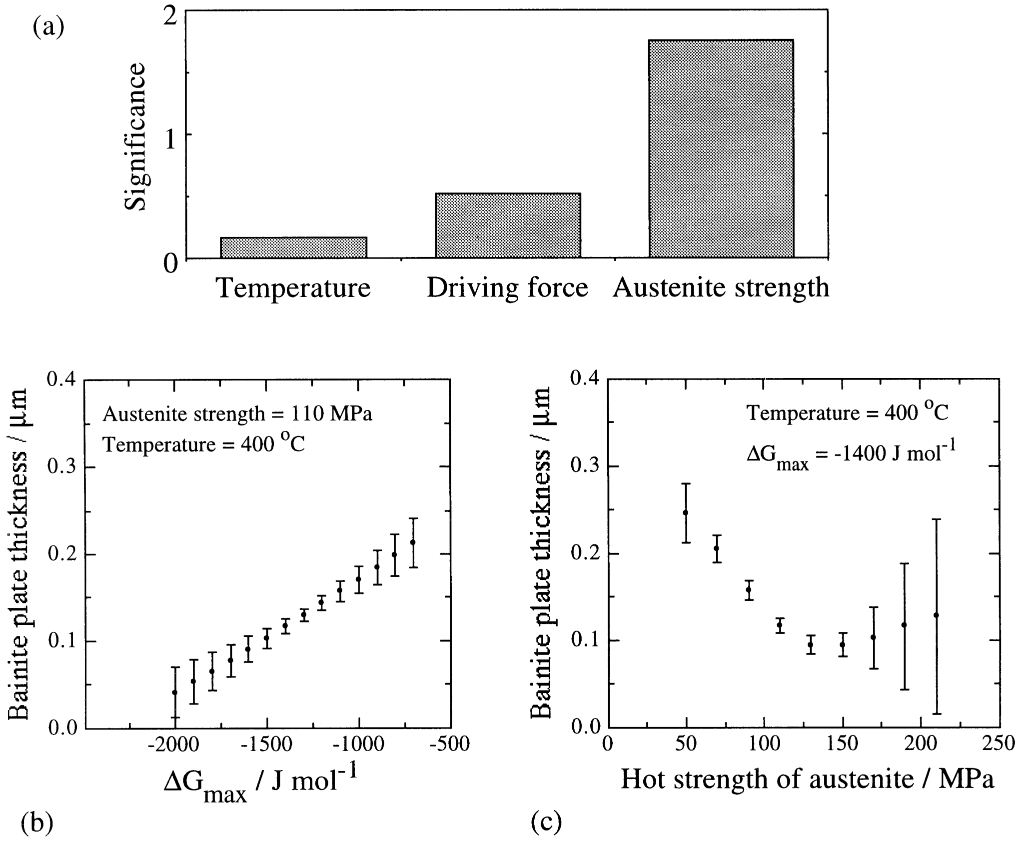

Fig. 2.7 (a) The model perceived significance of each of the variables plotted on the horizontal axis, in influencing the thickness of bainite plates. The vertical scale represents the ability of the variable to explain variations in plate thickness. (b) Variation in thickness with the chemical driving force. (c) Variation in thickness with the strength of the austenite. After Singh and Bhadeshia (1998).

2.1.3 Stereology

Crystals of bainite are anisotropic in shape. Their size is characterised by measuring the thickness on a random section in a direction normal to the long edges of the plates. The average value of many such measurements gives an apparent thickness which can be useful in correlations with mechanical properties. The true thickness requires stereological effects to be taken into account. If a plate is represented as a disc of radius r and thickness t with $r \gg t$, then the mean intercept length is given by $\overline{L}_3 = 2t$, and the mean intercept area is given by $\overline{A} = 2rt$ (Fullman, 1953). These intercepts must be taken at random.

The appropriate measure of the grain size is dependent on the application. For example, the strength will be a function of the dimensions of the slip planes within individual plates (Naylor, 1979; Daigne *et al.*, 1982). Assuming that there is a random distribution of slip plane orientations, the grain boundary strengthening term is of the form $\sigma_g = k_g M^{-1}$, where k_g is a constant and M is the mean value of the larger diameter of a slip plane. This differs from the Hall–Petch relation where it is the inverse square root of grain size which matters (Chapter 12).

2.2 Dislocation Density

Popular opinion is that bainite has a high dislocation density but there are few quantitative data to support this notion. Transmission electron microscopy has revealed a dislocation density ρ_d of about $4 \times 10^{14}\ \mathrm{m}^{-2}$ for an alloy with $B_S \simeq 650\,^\circ\mathrm{C}$. This compares with allotriomorphic ferrite obtained at 800°C in the same steel with $\rho_d \simeq 0.5 \times 10^{14}\ \mathrm{m}^{-2}$ (Smith, 1984). These data are similar to measurements on continuously cooled steel in which ρ_d {bainite} $\simeq 1.7 \times 10^{14}\,\mathrm{m}^{-2}$ and ρ_d{allotriomorphic ferrite} $\simeq 0.37 \times 10^{14}\,\mathrm{m}^{-2}$ (Graf *et al.*, 1985). It is significant that bainite contains more dislocations than allotriomorphic ferrite even when they form at similar temperatures.

The defect structure of bainite is often attributed to the shear transformation mechanism. However, such a mechanism need not lead to dislocations in the ferrite if the shape deformation is elastically accommodated. Thermoelasticity in martensites and shape memory alloys depends on the elastic accommodation of the shape deformation and the movement of any interfaces must occur without the creation of defects. It is only if the shape deformation is accompanied by plastic relaxation (Fig. 2.8), that the dislocations associated with this plastic strain are inherited by the product phase.

It is conceivable that the ferrite plate itself might relax. After all, the strength of both ferrite and austenite decreases at high temperatures. However, theory predicts that, for a plate shape, the strains are mostly accommodated in the austenite (Christian, 1965b, 1975). Hence, atomic-force microscope scans show that the displacements within the bainitic ferrite are much more regular than in the adjacent austenite (Fig. 2.8c). The plastic accommodation is more evident in Fig. 2.8d, where the strain is seen to extend into the austenite to a distance about equal to the width of the bainite.

Plastic relaxation has featured in many early observations. When polished samples of austenite are transformed to bainite, the adjacent austenite surface does not remain planar, but instead exhibits curvature which is characteristic of slip deformation (Srinivasan and Wayman, 1968b). Hot-stage transmission electron microscopy has shown that growth is accompanied by the formation of dislocations in and around the bainite (Nemoto, 1974). Direct observations

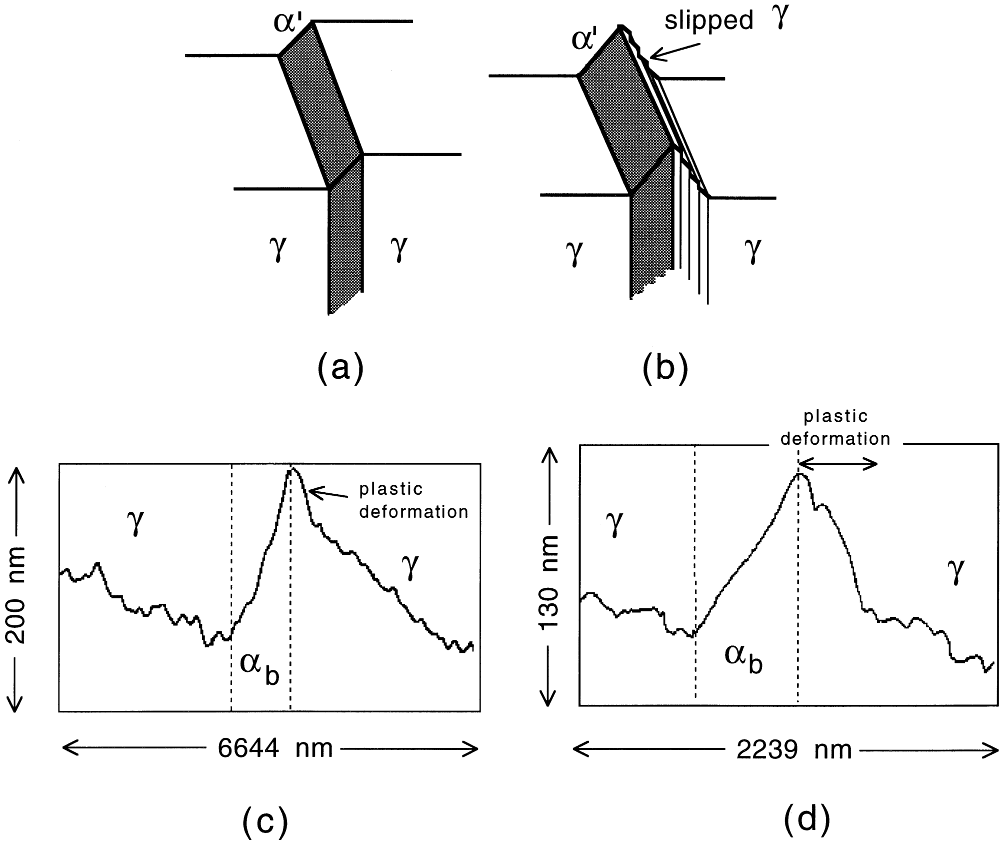

Fig. 2.8 (a) A perfect invariant-plane strain surface relief effect. (b) One where plastic relaxation of the shape change occurs in the adjacent matrix. (c,d) An actual atomic force microscope scan across the surface relief due to a bainite sub-unit (Swallow and Bhadeshia, 1996).

of the austenite/bainite interface show accommodation in both phases, Fig. 2.9. The austenite adjacent to the bainite can accommodate the shape deformation by mechanical twinning or faulting, with the density of defects increasing as the transformation temperature decreases (Bhadeshia and Edmonds, 1979a; Sandvik and Nevalainen, 1981; Sandvik, 1982a). These accommodation defects are common in martensitic transformations (Jana and Wayman, 1970).

The dislocation density of bainitic ferrite increases as the transformation temperature is reduced (Pickering, 1967). X-ray line profile measurements show an increase in the lattice strain due to dislocations as the transformation temperature is reduced. This can be used to estimate the dislocation density;

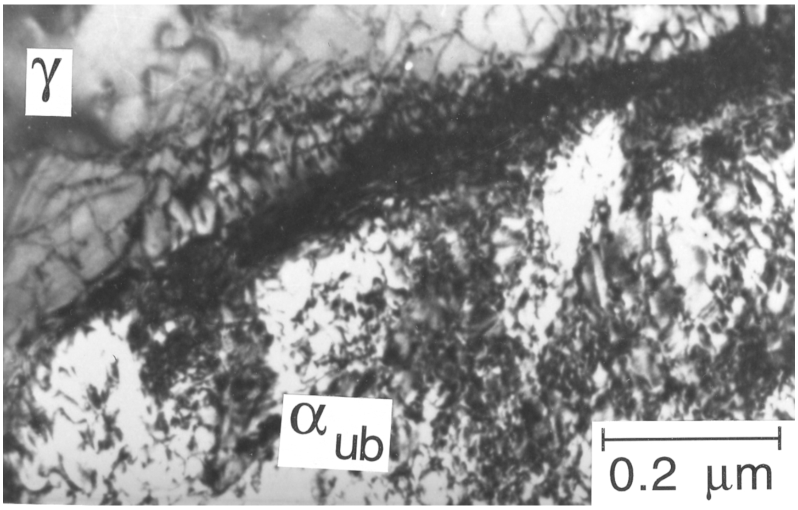

Fig. 2.9 Intense dislocation debris both at, and in the vicinity of the bainite/austenite transformation front (Bhadeshia and Edmonds, 1979a).

isothermal transformation to bainite at 300, 360 and 400 °C gave dislocation densities of 6.3×10^{15}, 4.7×10^{15} and $4.1 \times 10^{15}\,\mathrm{m}^{-2}$ respectively (Fondekar *et al.*, 1970).

2.2.1 *Quantitative Estimation of Dislocation Density*

It might be assumed that for low-alloy steels the dislocation density depends mainly on transformation temperature via the influence of the latter on the strength of the parent and product phases. It should then be possible to treat all of the displacive transformations, martensite, bainite and Widmanstätten ferrite together. This leads to an empirical relationship which is valid over the range 570–920 K (Fig. 2.10):

$$\log \rho_d = 9.28480 + \frac{6880}{T} - \frac{1780360}{T^2} \tag{2.1}$$

where ρ_d is the dislocation density in m^{-2}, and T is the reaction temperature in Kelvin (Takahashi and Bhadeshia, 1990). For martensite the transformation temperature is taken to be the M_S temperature. Although the dislocation densities of martensite measured by Norström (1976) are also plotted in the Fig. 2.10, those data were not used in deriving the expression because of uncertainties in the method used to assess the thickness of the thin foil samples used.

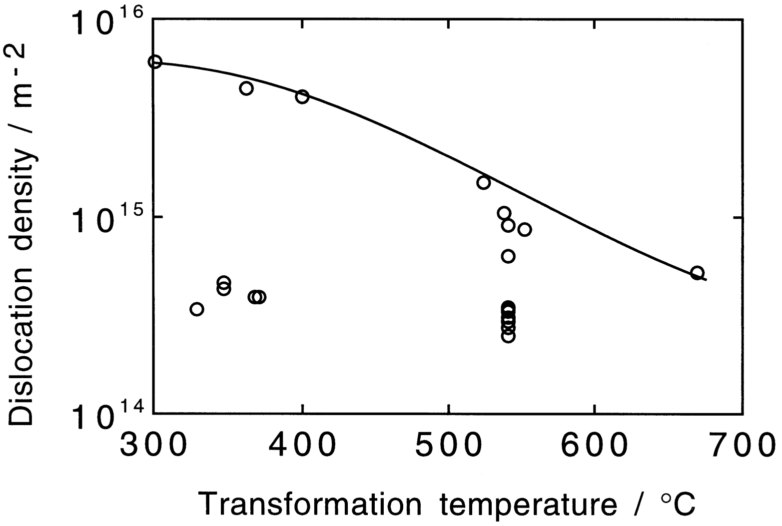

Fig. 2.10 Dislocation density of martensite, bainite, acicular ferrite and Widmanstätten ferrite as a function of the transformation temperature (Takahashi & Bhadeshia, 1990; Bhadeshia, 1997).

2.3 Chemical Composition

2.3.1 Substitutional Alloying Elements

There is no long-range redistribution of substitutional solutes during the growth of bainitic ferrite (e.g. Aaronson and Domain, 1966). High resolution experiments confirm this on the finest conceivable scale (Bhadeshia and Waugh, 1981, 1982; Stark *et al.*, 1988, 1990; Josefsson and Andren, 1988, 1989). The ratio of the iron to substitutional solute atoms remains constant everywhere during the formation of bainite. This is not surprising given the displacive character of the transformation and the low diffusivity of substitutional atoms at the temperatures where bainite forms. By contrast, all atoms, including iron must diffuse during a reconstructive transformation. Thus, it is possible to distinguish between a displacive and reconstructive mechanism even in pure iron.

A reconstructive transformation can be imagined to occur in two steps (Fig. 2.11): the change in crystal structure is achieved as in a displacive transformation; matter is then transferred in such a way that the shape deformation and strain energy associated with the first step is minimised. The matter must be transported over a distance about equal to the dimensions of the particle unless the interface is incoherent. This mass flow has been described as 'reconstructive diffusion' (Bhadeshia, 1985b).

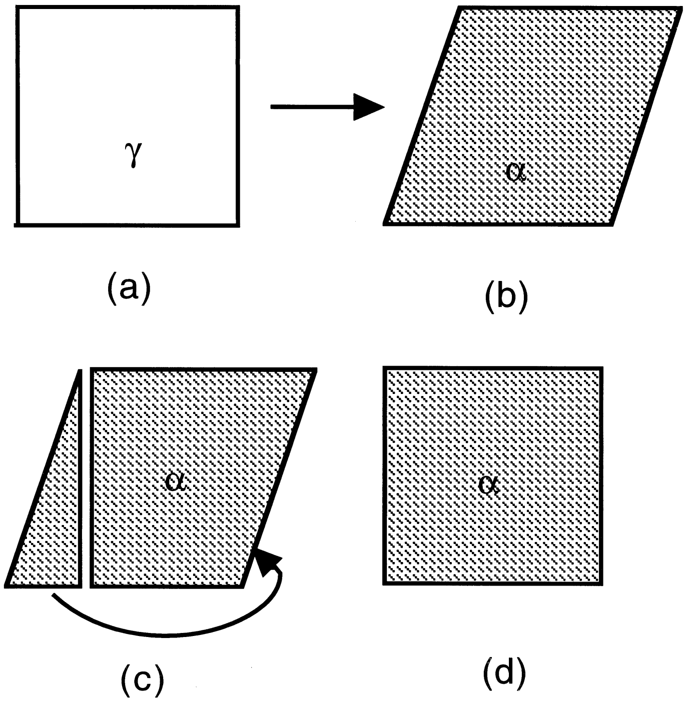

Fig. 2.11 Schematic illustration of the mass transport necessary to achieve reconstructive transformation, in both pure metals and alloys. Steps (a) to (b) represent displacive transformation, whereas (a) to (d) represent reconstructive transformation. The mass transport illustrated in (c) eliminates the shape change due to the shear.

The diffusion necessary for the lattice change provides an opportunity for the solvent and solute atoms to partition during transformation. In an alloy steel, the carbon atoms, which are in interstitial solution, can migrate at rates many orders of magnitude greater than the iron or substitutional solute atoms (Fig. 2.12). For diffusion-controlled growth the compositions at the transformation front are in local equilibrium, given by a tie-line of the phase diagram. However, the tie-line has to be chosen in such a way that both the carbon and the substitutional solute (X) can keep pace with the moving interface in spite of their vastly different diffusion coefficients. This can happen in two ways (Hillert, 1953; Kirkaldy, 1958; Purdy *et al.*, 1964; Coates, 1972, 1973a,b). First, the tie-line controlling the interface compositions is such that the gradient of carbon in the austenite is minimised (Fig. 2.13a). This is known as *partitioning, local equilibrium* or P–LE mode because there is the long-range partitioning of X. The P–LE mode of growth applies when the undercooling below the equilibrium transformation temperature is small.

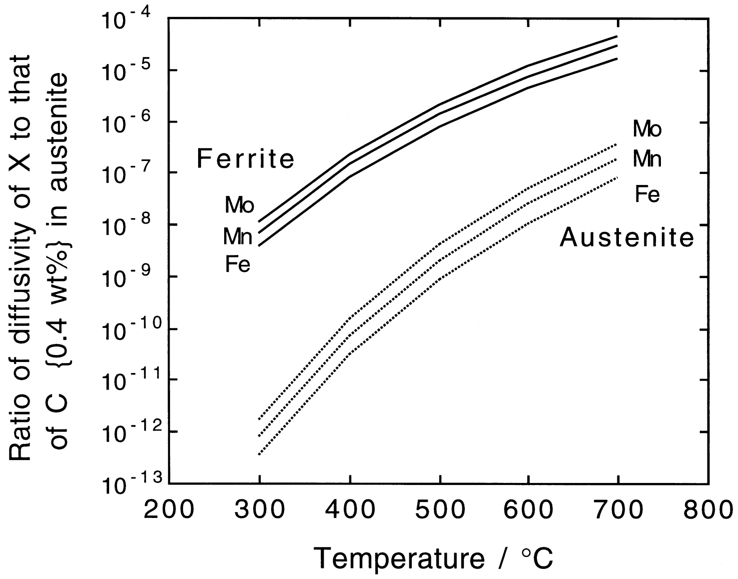

Fig. 2.12 A comparison of the diffusivities of iron and substitutional solutes relative to that of carbon (in austenite at a concentration of 0.4 wt%), in FCC and BCC iron, over the bainite transformation temperature range (data from Fridberg *et al.*,1969)

The second possibility is that a tie-line is selected so that the concentration gradient of X is large, thereby compensating for its small diffusivity (Fig. 2.13b). This is the *negligible partitioning local equilibrium* mode of transformation in which the ferrite has nearly the same X concentration as the austenite. This NP–LE mode occurs at large undercoolings below the equilibrium transformation temperature.

In the NP–LE mode, the concentration of X is uniform except for a small 'spike' in the parent phase adjacent to the interface. As the ratio of interstitial: substitutional diffusion rates increases, the width of this spike decreases, and when it becomes of the order of atomic dimensions, the concept of local equilibrium at the interface is invalid and has to be replaced (assuming the growth is nevertheless diffusion-controlled) by that of paraequilibrium (Hultgren, 1951; Rudberg, 1952; Aaronson *et al.*, 1966a,b). In conditions of paraequilibrium, there is no redistribution of Fe + X atoms between the phases, the Fe/X ratio remaining uniform right up to the interface. One interpretation of the paraequilibrium limit is that reconstructive transformation occurs with all displacements of the Fe + X atoms taking place in the incoherent interface; another interpretation might be that only displacive transformation can occur. In either case, to quote from Coates, 'the slow diffuser and the solvent

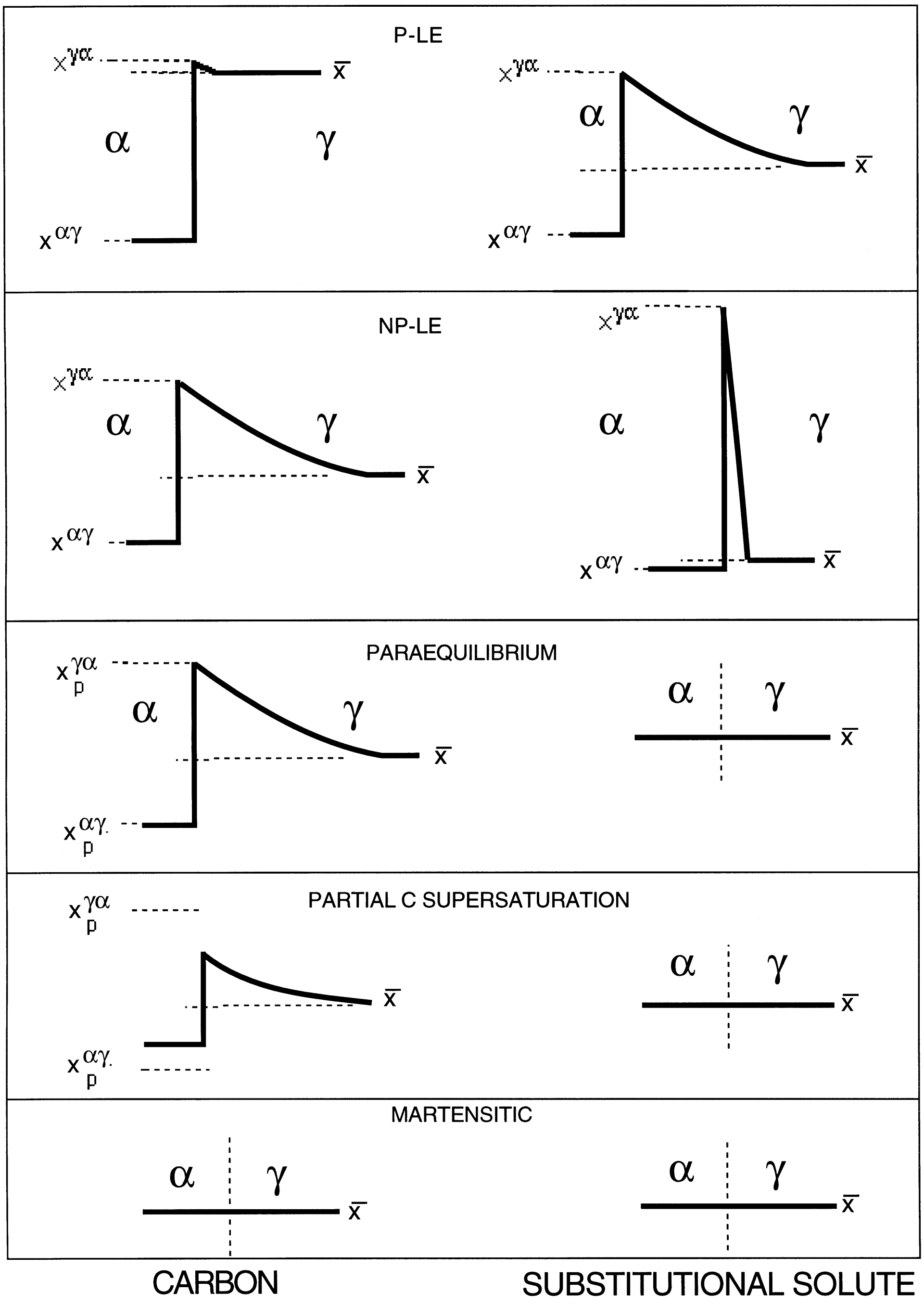

Fig. 2.13 The composition variations expected in the vicinity of the transformation interface, for a variety of growth mechanisms.

participate only in the change of crystal structure'. Paraequilibrium implies that a constant Fe:X ratio is maintained everywhere.

In conclusion, the experimental evidence that bainitic ferrite has the iron to substitutional atom ratio as its parent austenite is consistent with both reconstructive and displacive mechanisms for the change in crystal structure. However, reconstructive transformation with local equilibrium (or indeed any state between local and paraequilibrium) requires some perturbation of the substitutional solute content in the proximity of the interface. Experiments which have a chemical and spatial resolution on an atomic scale have all failed to show any evidence for the redistribution of alloying elements (Cr, Mn, Mo, Ni, Si) at the interface between bainitic ferrite and austenite, Fig. 2.14

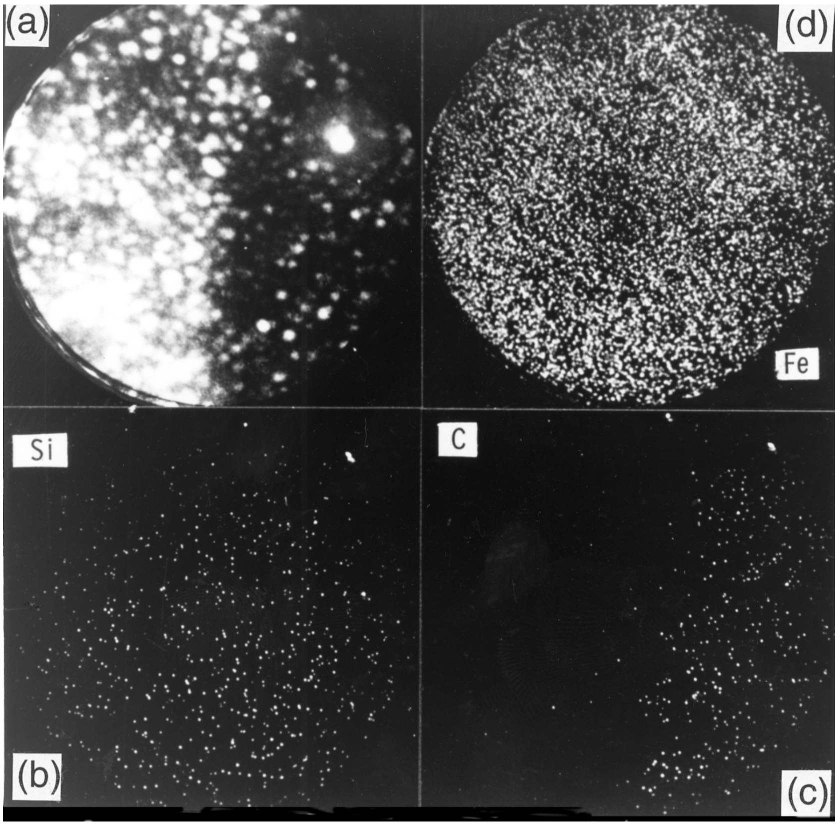

Fig. 2.14 Imaging atom-probe micrographs, taken across an austenite–bainitic ferrite interface in a Fe–C–Si–Mn alloy. The images confirm quantitative data (Bhadeshia and Waugh, 1982) showing the absence of any substitutional atom diffusion during transformation. (a) field-ion image; (b) corresponding silicon map; (c) corresponding carbon map; (d) corresponding iron map.

(Bhadeshia and Waugh, 1981, 1982; Stark *et al.*, 1988, 1990; Josefsson and Andren, 1988, 1989). These experiments were all based on steels where other reactions, such as the precipitation of carbides, do not interfere with the formation of bainitic ferrite. Measurements of the growth rates of grain boundary allotriomorphs of ferrite from austenite in alloy steels under conditions where bulk segregation is not observed (e.g. Kinsman and Aaronson, 1973; Bradley *et al.*, 1977) indicate calculated thicknesses of the spike of much less than 0.1 nm, and although these results are complicated by the effect of grain boundary diffusion, they are in general agreement with the concept that the lattice diffusion rate is inadequate to sustain local equilibrium at the growing interface. Only at temperatures above 600 °C, has the segregation of some (though by no means all) substitutional elements been obtained in grain boundary allotriomorphs (Aaronson and Domian, 1966b). Allotriomorphs are agreed to form by reconstructive mechanisms, but the absence of bulk segregation at moderately high transformation temperatures reinforces the belief, derived from the observed shape change, that bainitic ferrite forms at lower temperatures by a displacive rather than a reconstructive mechanism.

2.3.2 *Interstitial Alloying Elements*

A particular experimental difficulty with the bainite transformation is that in the case of upper bainite at least, it is almost impossible to say anything about the initial carbon content of the ferrite. This is because the time taken for any carbon to diffuse from the supersaturated ferrite into the austenite can be small. For the moment we refer to the interstitial content of bainitic ferrite *after* transformation. As will be seen later, the concentration *during* transformation is likely to be different.

Internal friction experiments indicate that the amount of carbon which associates with dislocations in bainitic ferrite increases as the transformation temperature decreases, but is independent of the average carbon concentration in the steel, at least in the range 0.1–0.4 wt%C (Pickering, 1967). This is consistent with the observation that the dislocation density of bainitic ferrite increases as the transformation temperature is reduced. The insensitivity to the carbon concentration is because most of the carbon ends up in the residual austenite. The results also show that at some stage during the evolution of bainitic ferrite, it must have contained a higher than equilibrium concentration of carbon.

These observations have been confirmed directly by using microanalysis on an imaging atom-probe, which has demonstrated quantitatively (Fig. 2.15) that the *post-transformation* carbon content of bainitic ferrite tends to be significantly higher than equilibrium (Bhadeshia and Waugh, 1982; Stark *et al.*, 1988, 1990; Josefsson and Andren, 1988, 1989). Precise electron diffraction experiments

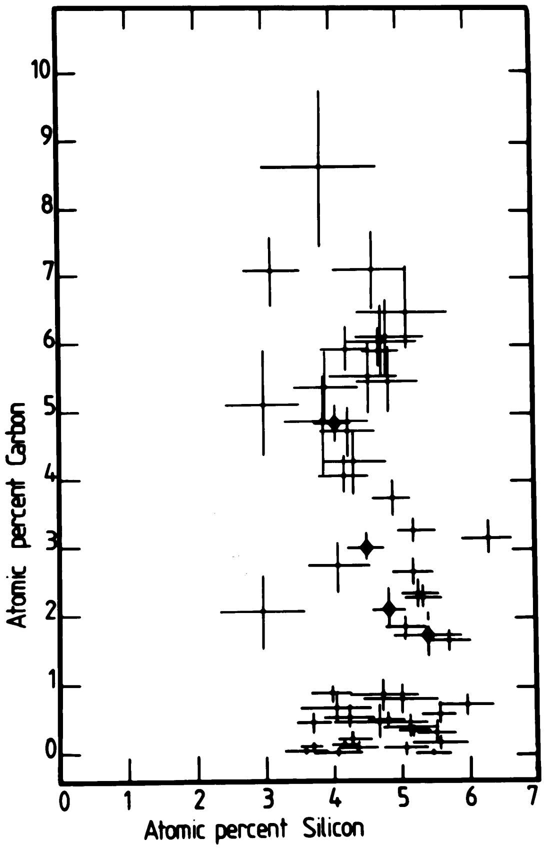

Fig. 2.15 Atom-probe determinations of the carbon and silicon concentrations of bainitic ferrite in an Fe–C–Mn–Si alloy transformed to upper bainite (Bhadeshia and Waugh, 1982). The average carbon concentration in the alloy is 1.93 at.%, so all concentrations below that level are measurements from bainitic ferrite.

using convergent beam Kikuchi lines to measure the lattice parameter of the bainitic ferrite also show that it contains a much larger concentration of carbon than expected from equilibrium (Zhang and Kelly, 1998a).

2.4 Crystallography

The properties of bainitic steels are believed to depend on the crystallographic texture that develops as a consequence of transformation from austenite. As an example, the ease with which slip deformation is transmitted across the adjacent plates of bainitic ferrite must be related to their relative orientation in space. Bainite grows in the form of clusters of plates called sheaves, with little misorientation between the plates within any given sheaf. Where they touch, adjacent plates are separated by low-misorientation grain boundaries.

The relative orientations of the bainitic ferrite and its parent austenite are always close to the classic KS (Kurdjumov–Sachs, 1930) and NW (Nishiyama–Wasserman, 1934) relationships (Fig. 2.16), although as will become evident later, they can never be exactly KS or NW. These two rational relations differ only by a relative rotation of 5.26° about the normal to the parallel close-packed planes of the two structures. The exact relative orientation is found in martensites to be intermediate and irrational, as is predicted by the crystallographic theory. High accuracy is required to compare theory with experiment since the predicted orientation relation is insensitive to input parameters such as lattice spacings or lattice invariant deformation. In the case of bainite, as in that of lath martensite, such precision is difficult to achieve partly because of the experimental difficulties in retaining austenite and partly because of the high dislocation densities.

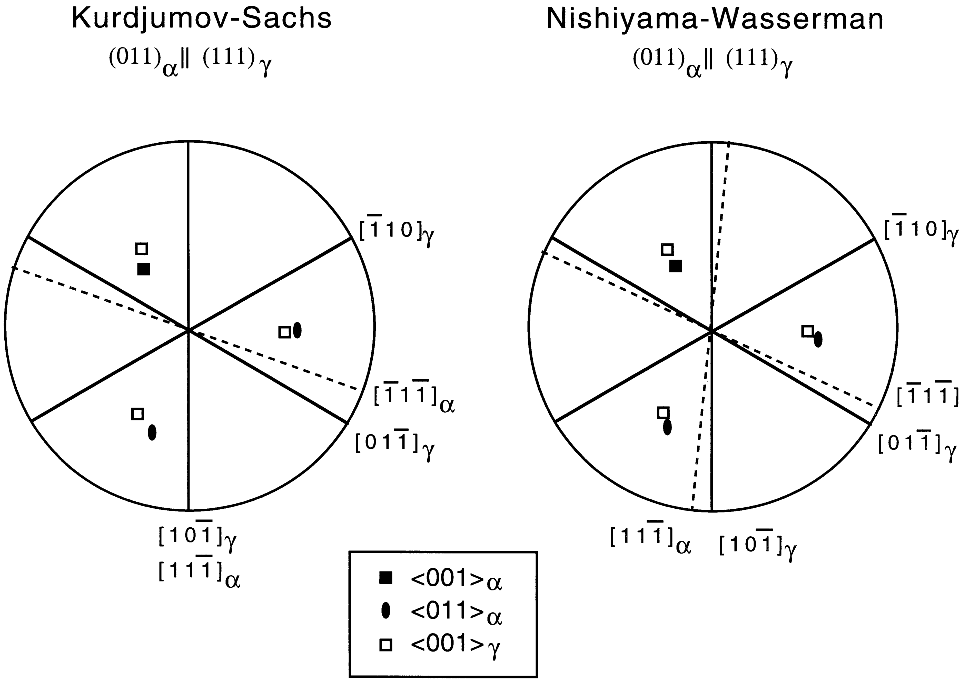

Fig. 2.16 Sterographic representation of the (a) Kurdjumov–Sachs and (b) Nishiyama–Wasserman orientation relationships. Note that NW can be generated from KS by a rotation of 5.26° about $[0\ 1\ 1]_\alpha$.

In spite of these difficulties, it is significant that the experimental data always lie well within the *Bain region* which encompasses the KS and NW relationships. The Bain strain is the pure part of the lattice deformation which for displacive transformations in steels converts austenite into ferrite or martensite (Fig 2.17, Bain, 1924). During the Bain strain, no plane or direction is rotated by more than 11° so that any pair of corresponding planes or directions may be made parallel by utilising a lattice deformation in which the Bain strain is combined with a rotation of not more than 11° (Crosky *et al.*, 1980). This

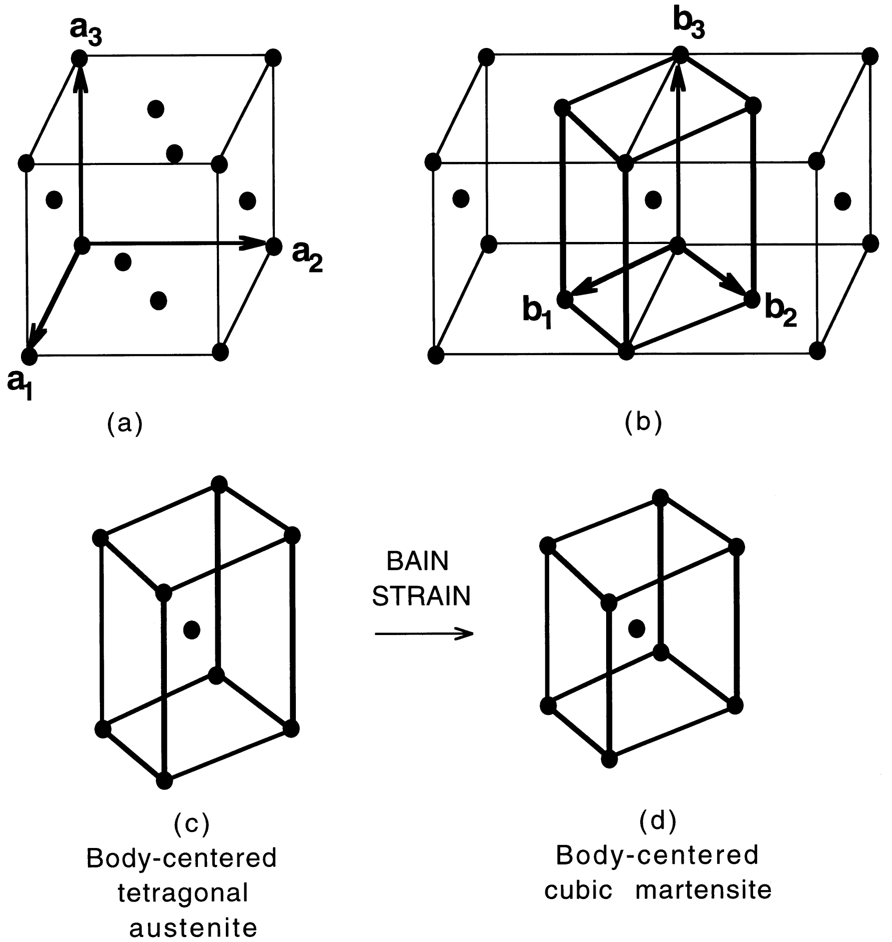

Fig. 2.17 (a) Conventional FCC unit cell of austenite, with basis vectors $\mathbf{a}_1, \mathbf{a}_2, \mathbf{a}_3$. (b) Relation between the FCC and body-centred tetragonal cell ($\mathbf{b}_1, \mathbf{b}_2, \mathbf{b}_3$) of austenite. (c,d) Bain Strain deforming the austenite lattice into a BCC martensite lattice.

defines the Bain region. The experimentally observed orientation relations are expected to lie within this region for displacive but not necessarily for reconstructive transformations. Thus, allotriomorphic ferrite is known to grow into austenite grains with which it has an orientation which is random or outside of the Bain region (King and Bell, 1975). It is therefore significant that bainitic ferrite always exhibits an orientation which is close to KS or NW and well within the Bain region.

There is an interesting consequence of the requirement that bainite must be within the Bain region of orientations. It is accepted that allotriomorphic ferrite, when it nucleates at an austenite grain surface, must also grow with an orientation relationship which is close to KS or NW in order to minimise the activation energy for nucleation. But allotriomorphic ferrite *grows* most rapidly along austenite grain boundaries with which it has a random orientation. Once nucleated, it therefore grows selectively, away from its original nucleation site. A grain of ferrite then has a large fraction of its interface with the austenite with which it has a random orientation. Bainite can only nucleate from allotriomorphic ferrite at the small fraction of interfaces where the orientation is in the Bain region (Fig. 2.18).

Pickering (1967) has suggested that the crystallography of bainite can be explained if the individual plates or laths adopt different variants of the NW or KS orientations, such that the ferrite orientations within a sheaf can be generated simply by rotation about the normal to a specific close-packed plane of the austenite. In this way, the bainite laths may nucleate side by side in rapid succession, the transformation strains determining the variant and hence the exact sequence. This early work was based on measurements of only ferrite–ferrite orientation relations, since the specimens may have contained only thin films of austenite which are observable only with high resolution microscopy. However, it must be admitted that results from more recent work in which measurements of the direct austenite–ferrite relations have been made are still contradictory. There is general agreement that adjacent plates or laths in bainite all have a $\{1\ 1\ 0\}_\alpha$ plane parallel (or almost parallel) to the same close-packed $\{1\ 1\ 1\}_\gamma$ and that the macroscopic habit plane is near to $\{1\ 1\ 1\}_\gamma$ in upper bainite but is irrational in lower bainite. Most investigators (e.g. Bhadeshia and Edmonds, 1980; Sandvik, 1982a) find all the plates within a sheath have a common orientation, but Sarikaya *et al.* (1986) claim that whilst some groups of adjacent laths have a common orientation, others have either different variants of the orientation relationship, or in lower bainite are twin-related. Similar discrepancies exist in crystallographic measurements on lath martensite where three types of orientation relation between adjacent laths of a packet are reported by some workers (Eterasivili *et al.*, 1979; Sarikaya *et al.*, 1986) and only one common orientation by others (Wakasa and Wayman, 1981; Sandvik and Wayman, 1983).

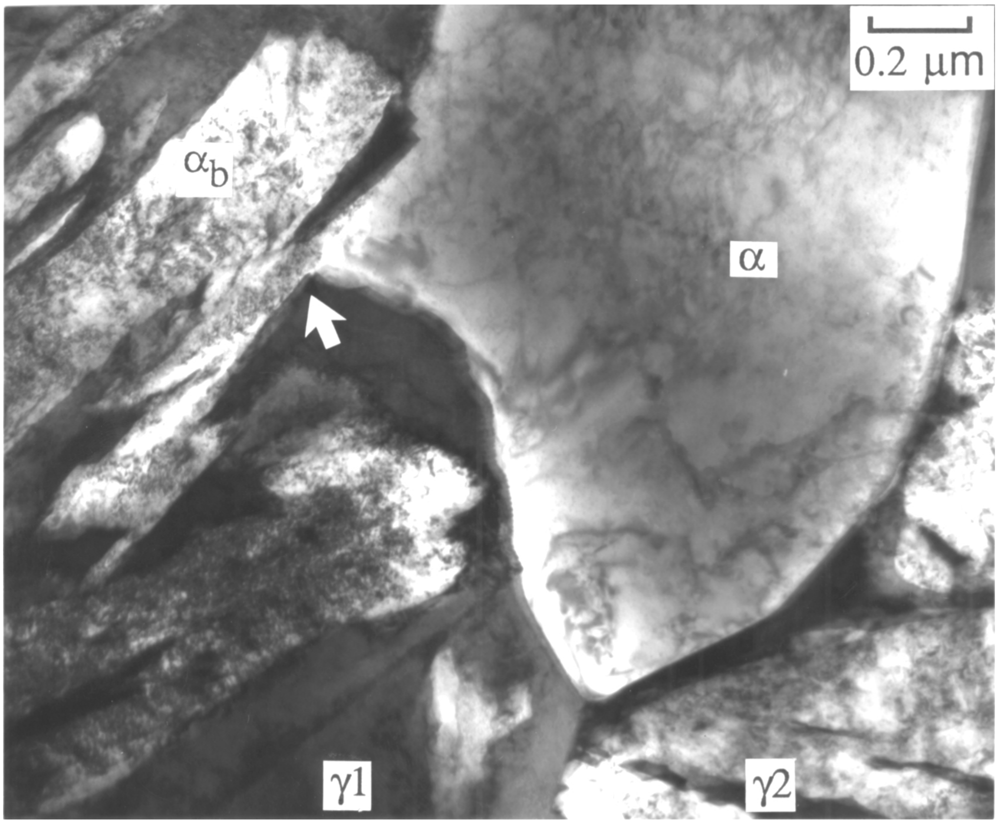

Fig. 2.18 Transmission electron micrograph showing an allotriomorph of ferrite at an austenite grain boundary. The allotriomorph is related to γ_1 by an orientation relationship which is close to KS, but is randomly orientated with respect to the lower grain. Consequently, a bainite plate has been able to nucleate from the allotriomorph only on the side where the orientation is suitable.

When there is a common orientation, the plates within a sheaf have small misorientations; there is also an appreciable spread of orientation within a single plate because of its high dislocation density. Direct crystallographic analysis indicates that all plates within a sheaf have an irrational orientation relation with the austenite which is closer to NW than to KS (Sandvik, 1982). Moreover, the shape deformations of all the plates are identical, Fig. 2.19, in agreement with earlier work (Srinivasan and Wayman, 1968b; Bhadeshia and Edmonds, 1980a). One further crystallographic observation made by Sandvik is of considerable interest. He found that twins formed in the austenite adjacent to the ferrite, and that the ferrite laths were able to grow through the twins, producing a reorientation of the lattice and also displacing the direction of the

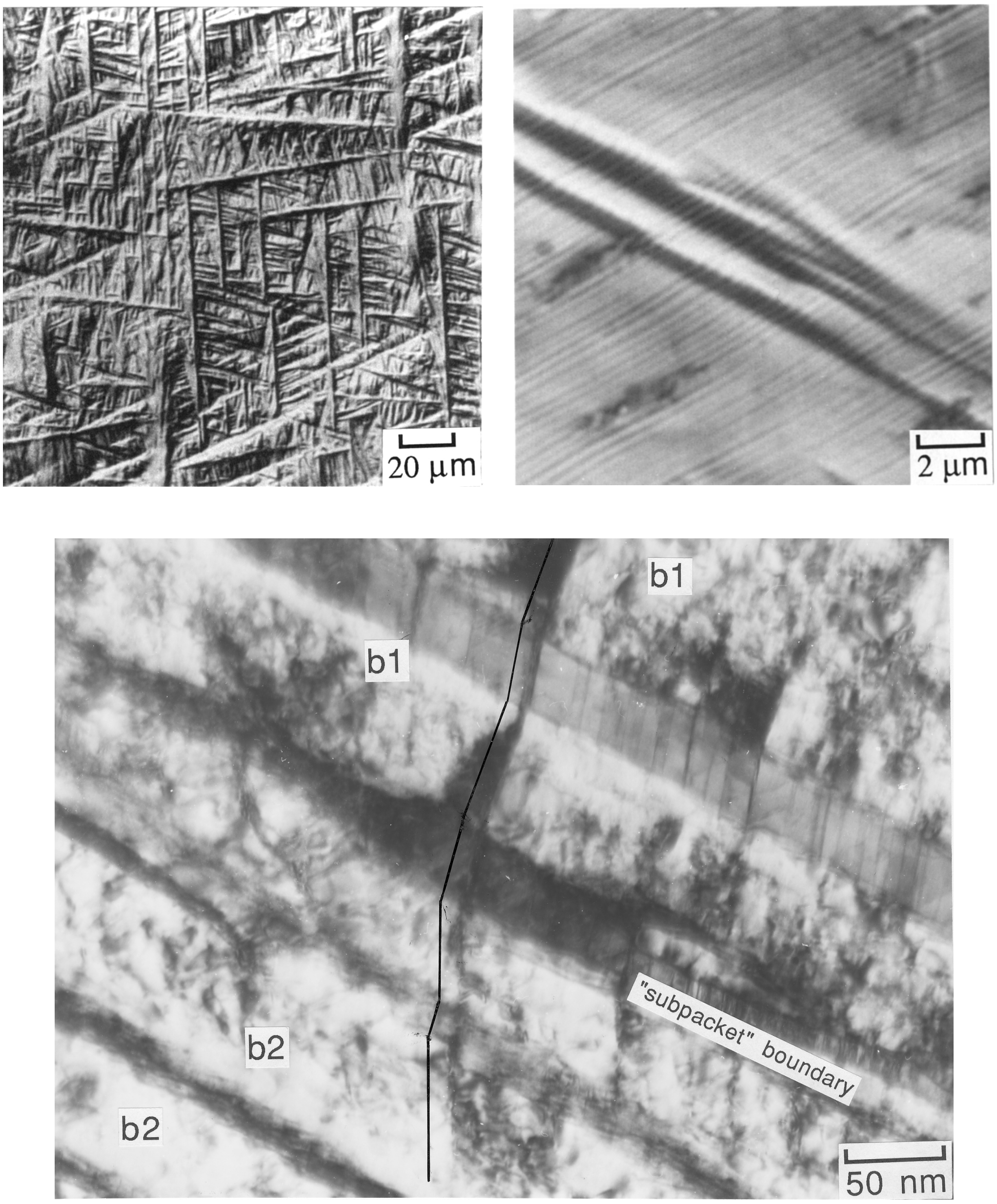

Fig. 2.19 (a) Nomarski differential interference contrast micrograph showing the general surface displacements due to upper bainite. (b) Higher magnification Nomarski image showing identical surface relief for all the sub-units within a given sheaf. (c) Sandvik's experiment showing the displacement of twin boundaries (parallel to the black line) caused by individual sub-units of bainite. The ferrite variants b1 and b2 belong to separate sheaves.

twin boundaries in the manner expected for a displacive (shear) transformation.

Similar results for the relative orientations of adjacent plates were obtained in a careful examination of lath martensite by Sandvik and Wayman, using an iron–nickel–manganese alloy which contained appreciable retained austenite (Sandvik and Wayman, 1983). They found that although the laths had slight relative misorientations of up to 2°, they all exhibited the same variant of the parent–matrix orientation relation, and thick layers of austenite between adjacent laths indicated that the laths did not form as a result of self accommodation of their shape strains. This form of lath martensite thus seems to be similar, in substructure at least, to the bainite investigated by Sandvik.

One possible reason for a common orientation might be that the individual plates of a sheaf are not separate crystals but are continuously connected portions of the growth front of one original nucleus. At the relatively high temperatures at which bainite (and lath martensite) form, the shape change may cause plastic deformation of the structure leading to copious generation of dislocations which stops the forward growth of a plate after it has attained a certain size. 'Nucleation' of a new plate would then simply be resumed growth caused by breakaway of a part of the original interface in a region near but not at the tip. In bainite, the growth would resume only after some carbon had been rejected from the ferrite into the austenite and would be most likely where pinning by dislocation debris is minimal and where the driving force is highest due to rapid dispersion of the carbon rejected to the austenite.

An alternative model is that the individual plates are completely separated from each other by thin layers of austenite, so that each is separately nucleated, but always in the same orientation. In general, the stress field at the tip will favour the same variant, whereas that at the side of the plate encourages an accommodating variant (Fig. 2.20).

Mutual accommodation of the shape deformation can occur between sheaves rather than between plates in each sheaf. Sandvik measured the misorientations between neighbouring sheaves and found that these correspond to different variants of his irrational orientation relation in which the same austenite {1 1 1} plane is parallel to a ferrite {1 1 0} plane. The six variants which satisfy this condition lead to four different relative orientations, one of which is only 3° from the original orientation and the others are respectively 8°, 11° and 14° away from a twin orientation. Sandvik comments that the first misorientation is difficult to detect, and that it is difficult to distinguish the remaining three from each other. He also comments that only the variant with orientation relation 14° from a twin relationship gives efficient self accommodation, and this was observed fairly infrequently. Adjacent sheaves are thus attributed to random association, although it is not clear why they should then all have the same pair of parallel close-packed planes. Sandvik and Nevalainen have also

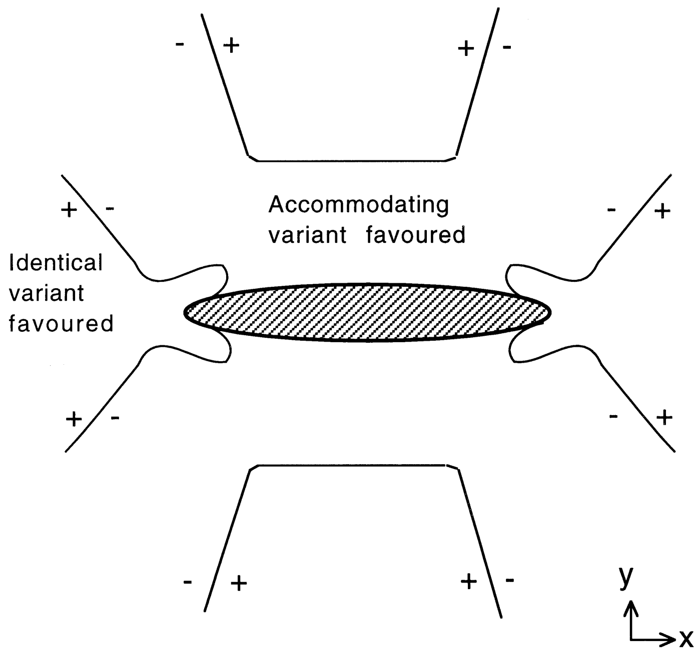

Fig. 2.20 Stress field contours of a martensitic particle lying in the xz plane with the transformation shear in the x direction. The positive signs represent regions where plates with the same shear direction are favoured, whereas the regions with the negative signs favour the formation of accommodating variants (Olson and Owen, 1976).

suggested that adjacent sheaves of bainitic ferrite are approximately twin related, and correspond to variants of a near NW orientation. Transmission electron microscopy by Josefsson (1989) has confirmed these observations in a Fe–Cr–Mo–C steel.

2.4.1 *Autocatalytic Nucleation*

Autocatalytic nucleation is a term commonly associated with martensitic transformations (Raghavan and Entwisle, 1965; Magee, 1970). The nucleation of martensite in steels is believed to begin at structural imperfections in the parent phase, such as arrays of dislocations. These are the preexisting defects which, on cooling below the M_S temperature dissociate into suitable partial dislocations in a way which leads to the nucleation of martensite (Olson and Cohen, 1976a–c). The defects are not all identical (they vary in potency) and are stimulated to grow into plates of martensite at different degrees of undercooling below the M_S temperature. This is the cause of the classical behaviour observed for athermal martensitic reactions, in which the volume fraction of martensite varies only with the undercooling below M_S.

The initial number density of preexisting defects typically found in austenite is not large enough to explain the kinetics of martensitic transformation. The extra defects necessary to account for the faster than expected transformation rates are attributed to autocatalysis: when plates of martensite form, they induce new embryos which are then available for further transformation. Three mechanisms have been proposed for autocatalysis (Olson and Cohen, 1981). In stress-assisted nucleation, the activation of less potent defects at a given temperature is induced by the internally generated elastic stresses arising as a consequence of the shape change due to transformation. In strain-induced autocatalysis, the creation of new and more potent nucleating defects is induced by some plastic accommodation in the parent phase. Finally, *interfacial autocatalysis* refers to the nucleation of new martensitic units from the existing martensite/austenite interfaces. Autocatalysis is responsible for the *bursts* of transformation (Fig. 2.21) that occur in certain martensitic steels,

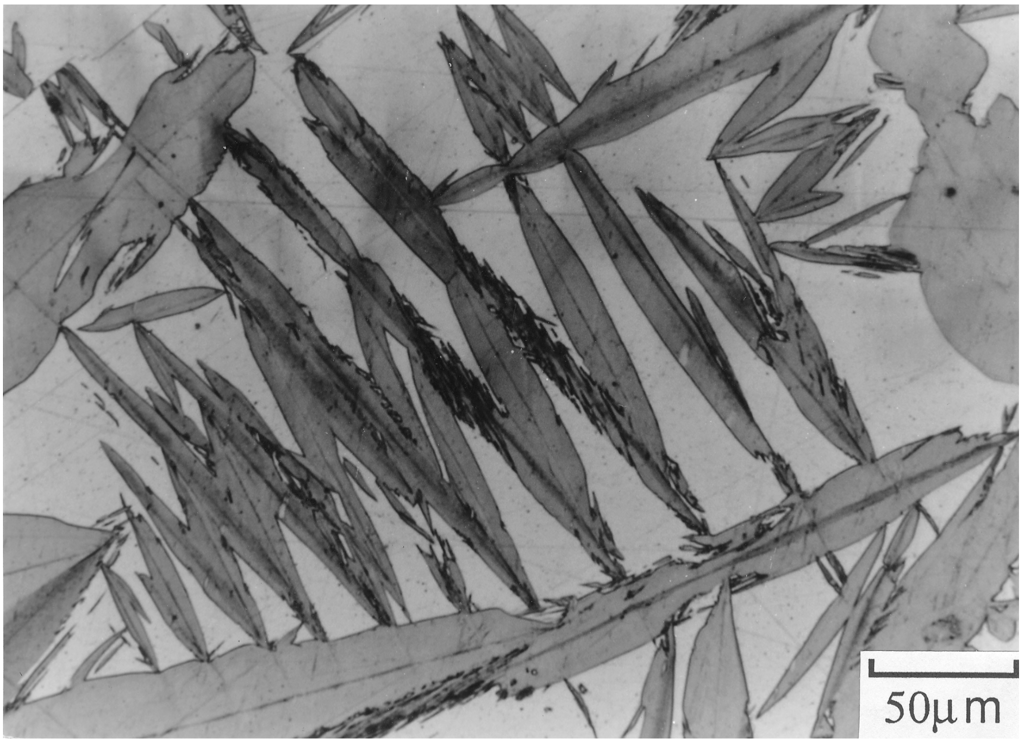

Fig. 2.21 A burst of autocatalytic martensitic transformation in a Fe–30Ni–0.31C wt% alloy. Such bursts are not observed during bainitic transformation.

whence the initial formation of a plate stimulates a disproportionately large degree of further transformation, sometimes causing the emission of audible clicks.

All of these effects arise as a consequence of the severe elastic and plastic disturbance of the austenite in the immediate vicinity of a plate of martensite. It is the shape change due to the martensitic transformation that is the cause of the disturbance. On this basis, autocatalysis should also feature prominently in bainitic transformations which are accompanied by similar shape deformations. There is, however, a significant difference in that bainite grows at relatively small driving forces, where defects induced by transformation do not seem to play as crucial a role in stimulating further nucleation. The initial nucleation event is almost always confined to the austenite grain surfaces, which presumably contain the most potent defects for nucleation. Intragranular nucleation of bainite can essentially be ignored except when nonmetallic particles may act as nucleation surfaces. The initial formation of a plate of bainite (or of a lath of martensite) must lead to appreciable elastic and plastic strains, but this does not seem to cause the nucleation of other plates in different orientations, as happens with plate martensite, and bursts of transformation are not observed. In the case of bainite, this may be because the driving force is only adequate for the formation of a carbon-free nucleus, and this may be impossible to form in the carbon-enriched region around an existing plate. Whatever the reason, it seems that strain-induced autocatalysis does not play an important role in bainite formation. As already discussed, there is some evidence for stress-assisted autocatalysis if it is indeed true that adjacent sheaves form in such a way as to help accommodate each other's shape deformation.

2.5 Crystallographic Theory

The deformation which converts the face-centred cubic structure of austenite to the body-centred cubic or body-centred tetragonal structure is known as the Bain Strain (Fig 2.17). Its principal deformation consists of a compression along the vertical axis $\mathbf{a}_3$ and a uniform expansion along $\mathbf{a}_1$ and $\mathbf{a}_2$. However, this deformation does not produce the experimentally observed orientation relationship; nor is it consistent with the observed invariant-plane strain shape deformation. An invariant-plane strain, on the other hand, cannot convert austenite into ferrite. The crystallographic theory, which resolves all of these difficulties, is now summarised (Wechsler *et al.*, 1953; Bowles and Mackenzie, 1954).

The Bain strain is a *pure* deformation because it leaves three mutually perpendicular directions unrotated, though distorted. The distortions η_i along these unrotated axes are defined as the ratios of the final to the initial lengths

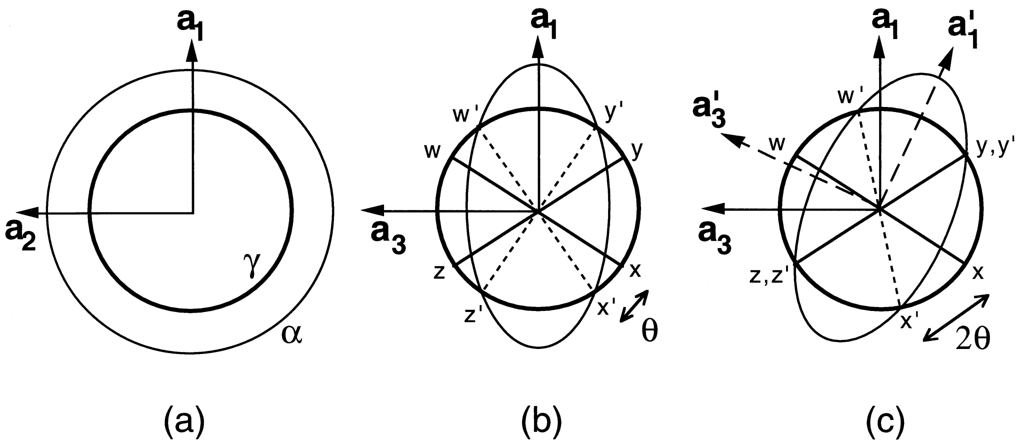

Fig. 2.22 (a) and (b) show the effect of the Bain strain on austenite, which when undeformed is represented as a sphere of diameter $wx = yz$ in three-dimensions. The strain transforms it to an ellipsoid of revolution. (c) shows the invariant-line strain obtained by combining the Bain strain with a rigid body rotation.

and are called the *principal distortions*. The Bain strain defines completely the lattice change so no further deformation is needed to complete the change in crystal structure.

Suppose that the austenite is represented by a sphere with its unit cell edges denoted by the vectors $\mathbf{a}_i$ with $i = 1, 2, 3$, as illustrated in Fig. 2.22a,b. The Bain strain changes the sphere into an ellipsoid of revolution about $\mathbf{a}_1$. There are no lines in the $(0\,0\,1)_\gamma$ plane which are undistorted. However, it is possible to find lines such as wx and yz which are undistorted by the deformation, but are rotated into the new positions $w'x'$ and $y'z'$. Since they are rotated by the Bain deformation they are not invariant-lines. In fact, the Bain strain does not produce an invariant-line strain (ILS). An invariant-line is necessary in the interface between the austenite and martensite in order to ensure a glissile interface.

The Bain strain can be converted into an invariant-line strain by adding a rigid body rotation as illustrated in Fig. 2.22c. The rotation reorients the α' lattice but has no effect on its crystal structure. The effect of the rotation is to make one of the original undistorted lines (in this case yz) invariant so that the total effect **RB** of the Bain strain **B** and the rotation **R** is indeed an invariant-line strain. This is the reason why the observed irrational orientation relationship (KS/NW type) differs from that implied by the Bain strain. The rotation required to convert **B** into an ILS precisely predicts the observed orientation from the Bain orientation.

It is apparent from Fig. 2.22c that there is no possible rotation which would convert **B** into an invariant-plane strain because there is no rotation capable of making two of the non-parallel undistorted lines into invariant-lines. Thus, it is impossible to convert austenite into α' martensite by a strain which is an invariant-plane strain. A corollary to this statement is that the two crystals cannot ever be joined at an interface which is fully coherent and stress-free.

It remains to resolve the inconsistency that **BR** is an ILS whereas the observed shape deformation is an IPS. The operations needed to explain this are illustrated in Fig. 2.23. When combined with an appropriate rigid body rotation, the net homogeneous lattice deformation **RB** is an invariant-line strain

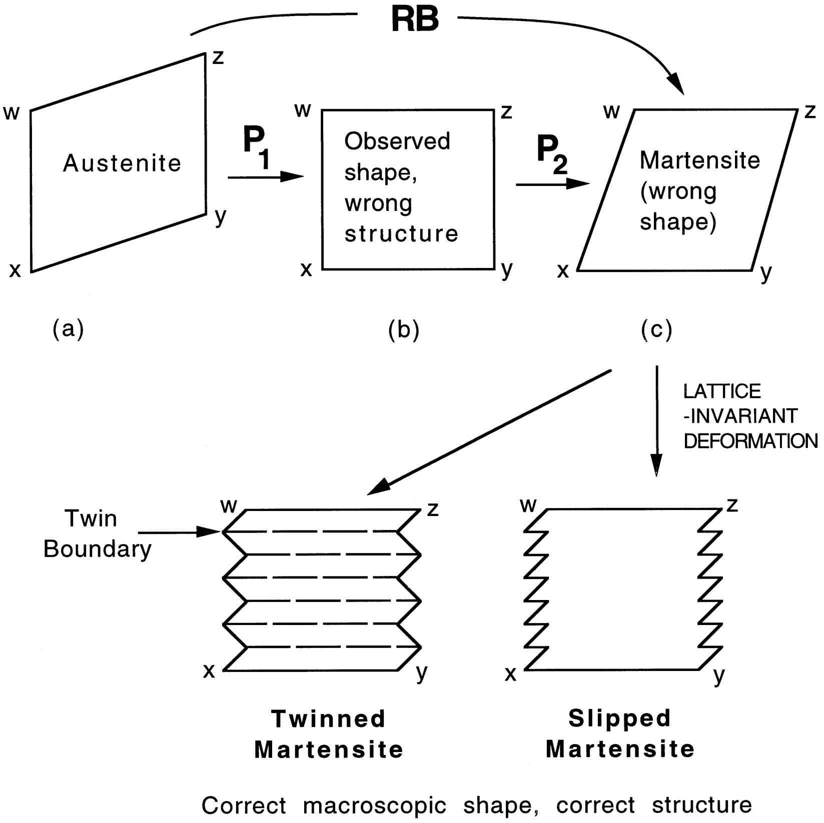

Fig. 2.23 The essential features of the phenomenological theory of martensite crystallography. (a) represents the austenite crystal and (c), (d) and (e) all have a body-centred cubic structure. (b) has an intermediate structure between FCC and BCC (or BCT). Although (c) has the BCC structure, its shape is inconsistent with the observed invariant-plane strain. The effect of the inhomogeneously applied lattice-invariant deformations is to correct the shape change to an IPS, without altering the structure.

(step a to c), the invariant-line being normal to the plane of the diagram and passing through the point x. Inconsistent with this, the observed shape deformation is an invariant-plane strain $\mathbf{P_1}$ (step a to b) but this gives the wrong crystal structure. The invariant-plane of the shape deformation is defined by xw. If, however, a second homogeneous shear $\mathbf{P_2}$ is combined with $\mathbf{P_1}$ (step b to c), then the correct structure is obtained but the wrong shape since[†]

$$\mathbf{P_1P_2} = \mathbf{RB}$$

The discrepancies are all resolved if the shape changing effect of $\mathbf{P_2}$ is cancelled macroscopically by an inhomogeneous lattice-invariant deformation, which may be slip or twinning as illustrated in Fig. 2.23. Notice that the habit plane in Fig. 2.23e,f is given by a fragmentation of the original plane xw, due to the inhomogeneous lattice-invariant shear. This is why the habit plane of martensite has peculiar indices. In the absence of a lattice-invariant deformation as in the $\gamma \rightarrow \epsilon$ transformation, the sequence stops at step b and therefore the habit plane has rational indices $\{1\,1\,1\}_{\gamma}$.

The theory neatly explains all the observed features of martensite crystallography. It is easy to predict the orientation relationship, by combining the Bain strain with a rigid body rotation which makes the net lattice deformation an invariant-line strain. The habit plane does not have rational indices because the amount of lattice-invariant deformation needed to recover the correct macroscopic shape is not usually rational. A substructure is predicted, consisting either of twins or slip steps, and this is observed experimentally. The transformation goes to all the trouble of ensuring that the shape deformation is macroscopically an invariant-plane strain because this reduces the strain energy when compared with the case where the shape deformation might be an invariant-line strain.

Finally, we note that the invariant-line lies at the intersection of the habit plane and the plane on which the lattice-invariant shear occurs. This is obvious since only the line common to the two invariant-planes can be invariant to their combined effect.

2.5.1 Application to Bainite

We have seen that the bainite transformation exhibits crystallographic features and surface relief effects identical to those associated with martensitic reactions. It is then natural to assume that the phenomenological theory of martensite crystallography should be applicable to bainite. The theory predicts

---

[†] Notice that a combination of two non-coplanar invariant-plane strains gives an invariant-line strain, the invariant-line lying at the intersection of the two invariant-planes.

a unique relationship between the habit plane, shape deformation, orientation relationship, lattice types and lattice-invariant deformation. It can be tested satisfactorily when all these variables are determined as a set. Much of the early data (reviewed by Bowles and Kenon, 1960) are incomplete in this sense, although consistent with the theory. The early measurements of habit planes must now be interpreted to refer to the habit planes of bainite sheaves, rather than of the individual plates.

A considerable difficulty in applying the theory to bainite is the lack of accurate structural information which is needed as input data. Thus if bainite grows with a full supersaturation but the carbon escapes in a short time, the measured lattice parameters of upper bainitic ferrite will not relate to the initially formed structure, which may even have been tetragonal. A problem exists for lower bainite if appreciable carbide precipitation has taken place before any measurements are possible.

Srinivasan and Wayman (1968b,c) reported the first detailed results on the crystallography of sheaves of lower bainite in a Fe–1.11C–7.9Cr wt% alloy ($B_S \simeq 300\,^\circ\mathrm{C}$, $M_S \simeq -34\,^\circ\mathrm{C}$) in which large quantities of austenite remained untransformed at ambient temperature. Each sheaf was found to have just one planar face when examined using light microscopy, and this was taken to be the habit plane. The irrational habit plane indices were found to exhibit a degree of scatter beyond experimental error, the mean indices being close to $(2\ 5\ 4)_\gamma$ relative to the orientation variant in which $(1\,1\,1)_\gamma$ is almost parallel to $(0\,1\,1)_\alpha$ and $[\bar{1}\,0\,1]_\gamma$ is at a small angle to $[\bar{1}\,\bar{1}\,1]_\alpha$; this is henceforth called the *standard variant*. The martensite habit plane in the same alloy is close to $(4\,9\,4)_\gamma$ and the difference in the two habits and in the exact orientation relations led Srinivasan and Wayman to the conclusion that the mode of displacive transformation is different in bainite and martensite. Their measured habit plane is only about 6° from that found for a different alloy by Sandvik, who pointed out that his result applied to an individual plate whereas that of Srinivasan and Wayman was for the average habit of a sheaf.

The shear component of the shape deformation, as averaged over the entire sheaf, was measured to be $\simeq 0.128$, the magnitude of the total shape strain being $\simeq 0.129$ (Table 2.1). This is consistent with the earlier data of Tsuya (1956) and Speich (1962). The actual shape strain for an individual sub-unit must of course be larger, and was estimated using crystallographic theory as being $\simeq 0.23$; this compares with the $\simeq 0.28$, 0.25 and 0.22 estimated for different alloys by Ohmori (1971a), Bhadeshia (1980a) and Sandvik (1982a) respectively. These values are in good agreement with a measurement of the shear component of the shape strain (0.22) of an individual sub-unit (Sandvik, 1982a) and with a value of 0.26 measured using atomic force microscopy (Swallow and Bhadeshia, 1996).

Table 2.1 Magnitude of the shape strain component parallel to the habit plane. The value of the shear is derived by measuring the tilts for each sheaf on two separate surfaces. After Wayman and Srinivasan (1969b).

Sheaf number	Tilt on surface 1	Tilt on surface 2	Angle of shape shear	Shear
1	5°48′	3°56′	7°9′	0.1254
2	5°24′	6°24′	8°27′	0.1486
3	5°17′	4°20′	7°0′	0.1228
4	6°45′	4°15′	7°55′	0.1393
5	6°9′	4°21′	8°20′	0.1466
6	3°43′	3°3′	5°13′	0.09156
7	4°15′	3°42′	8°24′	0.1474
8	4°0′	4°30′	6°	0.1035

Srinivasan and Wayman showed that their data on lower bainite are indeed consistent with solutions based on the phenomenological theory of martensite. The crystallography was, as expected, inconsistent with the lattice-invariant deformation being twinning since transformation twinning is not observed in bainitic ferrite.† It was found that the sheaf habit plane and orientation relationship could be predicted for an undistorted habit plane if it is assumed that the lattice invariant shear is irrational in both plane and direction. On the other hand, if the habit plane is permitted to undergo a small isotropic contraction, then the lattice-invariant shear (for the standard variant) consists of a double shear on the planes $(1\,\bar{1}\,1)_\gamma$ and $(1\,0\,1)_\gamma$ in the common direction $[\bar{1}\,0\,1]_\gamma$ (these correspond to $(1\,0\,1)_\alpha$, $(1\,1\,2)_\alpha$ and $[\bar{1}\,\bar{1}\,1]_\alpha$ respectively). This double system is equivalent to a single shear on an irrational plane, and is not associated with any of the difficulties encountered in theories which postulate more general combinations of lattice-invariant shears. The component planes on which the interface dislocations would glide are those most usually considered as candidates for single lattice-invariant shears in the martensite theory. However, at the time of the Srinivasan and Wayman work, it was not fully appreciated that the so-called habit plane of a sheaf which they measured, may differ from that of a plate within a sheaf which Sandvik measured, and it is not yet clear whether the phenomenological theory of martensite should be applied to the sheaf or the plate. It may be more important to minimise long-range distortions over the whole sheaf, in which case the invariant plane condition would apply to the apparent habit plane of the sheaf, but in cases where there are reasonably thick layers of austenite between the plates, it seems more logical to apply the theory to the individual plate.

2.5.2 *High-Resolution Studies of the Shape Change*

Of the transformation products listed in Table 2.2, both Widmanstätten ferrite and martensite can be obtained in the form of plates that are readily resolved using optical microscopy. Their shape deformations have been known for many decades, the measurements being made from the deflection of scratches or optical interference fringes on a surface polished flat prior to transformation.

Table 2.2 Approximate values of the shear strain *s* and dilatational strain δ for a variety of transformation products in steels.

Transformation	***s***	δ	**Morphology**	**Reference**
Widmanstätten ferrite	0.36	0.03	Thin plates	Watson & McDougall, 1973
Bainite	0.22	0.03	Thin plates	Sandvik, 1982a
	0.26		Thin plates	Swallow & Bhadeshia, 1996
Martensite	0.24	0.03	Thin plates	Dunne & Wayman, 1971
Allotriomorphic α	0	0.03	irregular	
Idiomorphic α	0	0.03	equiaxed	

However, the microstructure of bainite consists of fine plates of ferrite, each of which is only some 0.2 μm thick, which is below the limit of resolution in light microscopy. This has made it difficult to establish the surface relief introduced as bainite grows. Sandvik (1982a) first measured the shear strain of a single bainite plate using transmission electron microscopy to reveal the transformation-induced deflection of twins in austenite. He determined the shear strain *s* to be close to 0.22.

New methods have recently become available for the quantitative, high-resolution measurement of surface topography using scanning tunnelling or atomic force microscopy. The techniques have confirmed Sandvik's observations which revealed that the shear strain associated with an individual plate of bainite is about 0.26 ± 0.02 which is consistent with the magnitude expected from the phenomenological theory of martensite crystallography (Swallow and Bhadeshia, 1996). An example of an image of the surface displacements is presented in Fig. 2.24.

[†] A twinned interface is never thermodynamically favoured because of the creation of internal twin boundaries. But it can move more rapidly than when slip is the lattice-invariant deformation mode. Consequently, martensite which grows at high velocities will tend to contain transformation twins (Olson and Cohen, 1981b).

The atomic force microscopy has also shown that the low values of s measured in early work using light microscopy arise because the low resolution causes an averaging of the shape strain over the sheaf.

The plastic relaxation is of course, ultimately responsible for the arrest in the growth of the bainite plates, giving the sub-unit and sheaf hierarchies in the microstructure of bainite; as discussed in section 2.2.1, it also leads to an increase in the dislocation density of the bainite.

2.5.3 The Shape Change: Further Considerations

In talking about the application of the phenomenological theory of martensite to bainite, the classical view (Hull, 1954; Bilby and Christian, 1956; Christian, 1962) that the experimentally observed invariant-plane strain shape deformation implies a coordinated movement of at least the iron and substitutional atoms was implicitly accepted. Given that there has been some confusion in the literature about the interpretation of this shape change, it is worth presenting an assessment of the significance of the shape change (Christian and Edmonds, 1984; Christian, 1990a). The problem is important since the strain energy associated with the shape deformation when transformation occurs under constraint, cannot be ignored in the thermodynamic and kinetic descriptions of bainitic reactions, irrespective of the mechanism by which the shape change is proposed to arise.

The intersection of a plate of bainitic ferrite with a free surface causes that surface to tilt about the lines of intersection. This is the description of an invariant-plane strain, which is due to the combined effects of the lattice deformation and a lattice-invariant deformation. The tilting produced is homogeneous on a macroscopic scale, indicating that the net atomic displacements include common non-random components which accumulate during growth. This is an obvious conclusion, but the term *net atomic displacements* needs to be deconvoluted in order to assess the degree of diffusion which can be tolerated before the transformation must be regarded as a reconstructive reaction.

Focusing attention on equivalent lattice points which define unit cells (not necessarily primitive) of the two structures containing the same number of atoms, a change in shape will accompany transformation if the new set of lattice points can be related to the original set by a homogeneous deformation. It is then possible to specify (in a localised region at least) how particular vectors, planes and unit cells of one structure are derived from *corresponding* vectors, planes and unit cells of the other structure. This is termed a lattice correspondence and it defines the pure lattice deformation which carries the original lattice points, or some fraction of those points into points of the new lattice.

When interstitial atoms are present, they may move over large distances without affecting the correspondence; this is sometimes expressed by stating that there is an atomic correspondence for the solvent and substitutional solute atoms but not for the interstitials. A further relaxation of the condition is to allow the solvent and substitutional solute atoms to be displaced during transformation among the sites specified by the lattice correspondence, but not to create new sites or destroy any specified sites; in this way the lattice correspondence is preserved but there is no longer an atomic correspondence. Thus, a systematic shape change implies a lattice correspondence even if accompanied by some diffusion of atomic species. As will become evident later, the existence of this correspondence and the shape change requires an interface which is at least semi-coherent.

The detailed implications of the shape change on the mechanism of growth can be illustrated using the virtual operations illustrated in Fig. 2.25. A region of the matrix is first removed (leaving behind an equivalent hole) and then

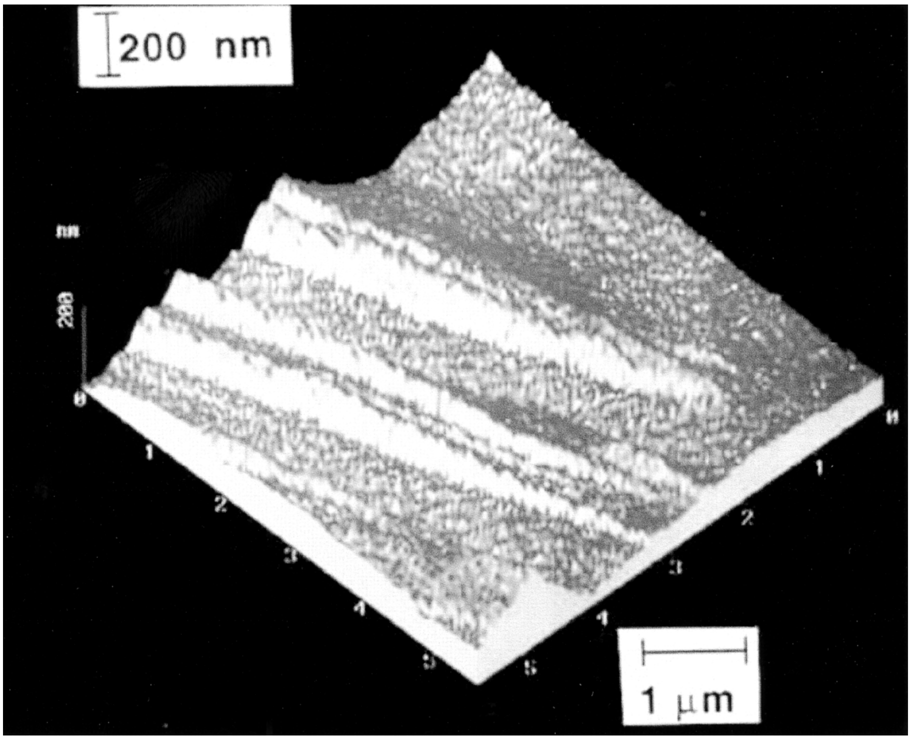

Fig. 2.24 High-resolution atomic-force microscope plot of the displacements caused by the formation of a single sub-unit of bainite. The surface was flat before transformation. Note the plastic deformation caused in the adjacent austenite (Swallow and Bhadeshia, 1996).

allowed to undergo unconstrained transformation with the help of a homogeneous lattice deformation which is not in general an invariant-plane strain (Fig. 2.25a,b). The particle is then allowed to have any required composition by transferring suitable numbers of solute atoms between interstitial sites in the particle and the matrix, and/or by interchanging atoms of substitutional species in the particle with atoms in the matrix (operation c, Fig. 2.25).

A number of further operations are now possible before the particle is reinserted into the hole in the matrix, in order to reduce the strain energy:

(i) The volume and shape of the particle may be made equal to that of the hole, by transferring atoms over long distances from the particle to sinks within the matrix or at its surface (operation d_1, Fig. 2.25). The strain energy then vanishes.

(ii) The total number of atoms in the particle may be conserved but its shape may nevertheless be adjusted by the creation and removal of atom sites. The strain energy is effectively that of a hole in the matrix filled with a compressible fluid of different natural volume. For a plate-shaped particle, the minimum in strain energy for this case corresponds to an IPS with a zero shear component, with the expansion or contraction being normal to the habit plane (operation d_2, Fig. 2.25). A plate-shaped particle will give the lowest strain energy if the volume change is appreciable, but there will only be a *preferred* habit plane if there is appreciable anisotropy of either the elastic properties or the interfacial energy.

(iii) The shape of the particle may be changed by conservative plastic deformation. The lowest strain energy for a plate-shaped particle then occurs if the plastic deformation converts the lattice deformation into a shape deformation which is an IPS on the habit plane, as in the theory of martensite crystallography (operation d_3, Fig. 2.25).

(iv) The shape of an epitaxially coherent particle (which has interfacial dislocations with Burger's vectors which have an edge character and which lie in the interface plane) may be changed by the removal or addition of particular planes of atoms, e.g. by dislocation climb from one surface to another, again giving lowest strain energy for an IPS on the habit plane of a plate precipitate. If there is no reconstruction of the atom sites, the shape change may retain an appreciable shear component (operation d_4, Fig. 2.25).

Particles of type d_1 and d_2 both require long range diffusion or mass transport, and there is no obvious reason why large scale redistributions of solute atoms cannot at the same time occur between the product and parent phases, if demanded by thermodynamic equilibrium. In d_1 there is no shape change,

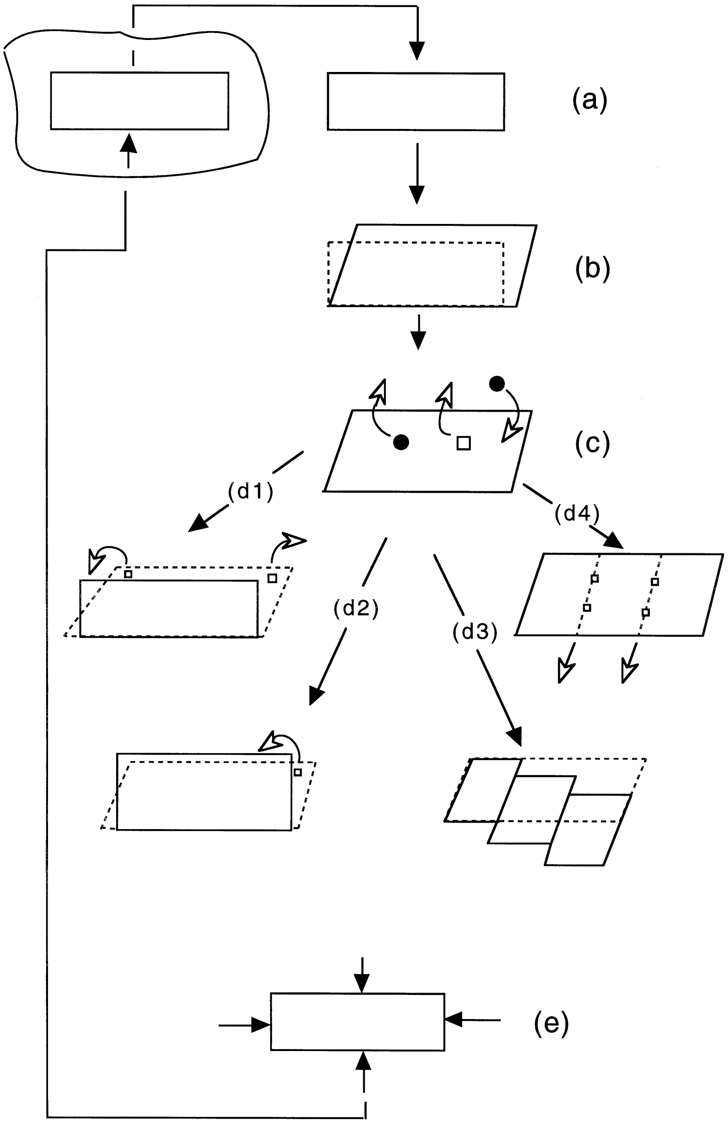

Fig. 2.25 Schematic diagram illustrating the virtual operations required to form a particle in a constraining matrix (after Christian and Edmonds, 1984).

whereas d_2 will lead to surface rumpling due to the volume change accompanying transformation; both of these kinds of transformation are therefore reconstructive. Shear stresses and strains are not transferred across the interface, which behaves in some respects as a liquid-like layer. Since there is no continuity of planes or vectors, the interface can be displaced only as a result of individual atomic migration and its velocity will depend on atomic mobility.

It could also be argued that in case (iv), the need to have sufficient atomic mobility for interfacial dislocations to climb means that in reality, other diffusion processes might also occur which remove the shear component of the shape deformation (Christian, 1962).

This leaves only the martensitic type change (iii) as a likely candidate for an IPS shape change, but step *c* (Fig. 2.25) ensures that the shape change cannot be taken to imply diffusionless transformation. It is easy to see how interstitial atoms can partition between the phases during growth without affecting the IPS shape change. There may also be an interchange of substitutional atoms (of the type necessary to induce ordering in equiatomic random alloys), but it is likely that the migration of these atoms can only occur over a few interatomic distances – otherwise, any longer range diffusion would destroy the shape change and its associated strain energy at the same time. It is therefore to be concluded that one implication of the observation of an invariant-plane strain shape change with a significant shear component is that any diffusion of solvent or substitutional atoms during transformation must be absent or minimal.

Suppose that there is an IPS deformation with a large shear and at the same time there is a composition change implying diffusion in the substitutional lattice. Such a transformation has been called diffusional–displacive transformation (Christian, 1994; 1997). This does not negate the consequences of the shape deformation, for example the strain energy, the plate shape, the requirement for a glissile interface etc. The existence of the shape deformation means that the diffusion flux is not adequate to eliminate the displacive character of the transformation, and furthermore, the fact that most of the atoms must move in a coordinated manner to produce the displacements in the first place. It is a mistake to imagine that the association of diffusion with a phase transformation means that it can be treated as a reconstructive reaction which is close to equilibrium. The IPS shape deformation with its shear therefore remains evidence for the displacive character of the transformation mechanism when the atomic mobility is clearly inadequate to permit the elimination of the shape deformation.

Further implications of the shape change become clear when its relationship with the interfacial structure is considered. The interface in cases (iii) and (iv) is semicoherent because for coherency $\mathbf{RB} = \mathbf{P}$, an equation which is rarely satisfied in general, and not satisfied for the FCC to BCC or BCT transformation in steels. For the epitaxial semicoherency illustrated in (iv), coherent patches on the invariant-plane are separated by interface dislocations whose motion with the interface requires climb and hence diffusion of atoms in substitutional sites. The semicoherent interface may alternatively be glissile; the interface dislocations then glide conservatively as the interface moves and growth does not require diffusion and hence has a high mobility even at low temperatures (case iii). For ferrous bainites, the mobility of the solvent and substitutional atoms is negligible, and the experimental observation of a shape deformation with a significant shear component gives strong evidence that the bainitic–ferrite/austenite interface is semi-coherent and glissile.

2.5.4 *The Shape Change and the Superledge Mechanism*

The lattice correspondence that is implied by the IPS shape deformation is a relationship between the lattices of the parent and product phases, independent of the orientation of the actual interface between the enclosed particle and the matrix. It follows that all the interfaces surrounding an enclosed particle of bainitic ferrite must be semicoherent (Christian, 1990a). It is not tenable to consider some interface orientations to be incoherent ('disordered') while semi-coherency is maintained on other interface orientations, as is sometimes implied in the superledge mechanism of bainitic growth (Aaronson *et al.*, 1970). This mechanism considers that the growth of bainitic ferrite plates occurs by the propagation of macroscopic ledges on the habit plane. The model requires at least two differently oriented macroscopic interfaces around an enclosed bainitic ferrite particle, the invariant-plane and the superledge. Macroscopic interfaces like these can only exist if the distortion due to the coherency between the parent and product lattices is within an elastically tolerable range, i.e. if the shape deformation across the interface is a close approximation to an IPS. Thus, the presence of two different orientations of macroscopic interface means that there are two invariant-planes between the parent and product crystals, a situation only possible if the net shape deformation is zero, in contradiction with experimental evidence.

All interface orientations other than the invariant-plane of the observed IPS shape deformation (which is also the habit plane of the bainitic ferrite) must be small coherent steps in the semi-coherent habit plane interface. The small steps are in forced *coherency* with the matrix, and have the characteristics of transformation dislocations which can glide and climb conservatively (also called coherency dislocations, Olson and Cohen, 1979). Coherency implies that all the corresponding planes and lines are continuous across the step; thus, these transformation dislocations are not lattice discontinuities. There is therefore no difficulty in these transformation dislocations climbing and gliding conservatively even when the Burgers vector is not parallel to the line vector.[†] The strain energy associated with the small steps is tolerable only because of their

---

[†] The terms transformation dislocation and coherency dislocation are identical. They are distinct from the adjectives 'interface', 'intrinsic', 'misfit' and 'anticoherency', all of which are used to describe dislocations which form an intrinsic part of the boundary structure (Olson and Cohen, 1979; Christian, 1990a).

small size. It is therefore considered that large steps (or 'superledges') are most improbable because of their high strain energy (Christian, 1990a).

2.5.5 *The Structure of the Interface*

It has already been pointed out that any atomic height steps in the bainitic/austenite interface are transformation dislocations, with strain fields whose character can be specified by assigning a Burgers vector to each such dislocation. The motion of these steps (or coherency dislocations) which are in forced coherency, leads to phase change: there is continuity of planes and vectors across the steps so that regions of the parent lattice are homogeneously deformed into that of the product as the steps are displaced. Since the energy of the step varies with the square of the magnitude of its Burgers vector, the step is restricted to atomic height, which is another way of stating that superledges are impossible on a bainitic/austenite interface. The anticoherency or interface dislocations cause the lattice-invariant deformation as the interface is displaced.

There are no decisive observations of the structure of the bainitic ferrite/austenite interface, but general conclusions can nevertheless be deduced using other experimental data and theoretical considerations. The observation of an invariant-plane strain shape change accompanying the growth of bainitic ferrite, when combined with the negligible mobility of the solvent and substitutional solute atoms, provides strong evidence that the structure of the transformation interface must be glissile. The number of iron and substitutional solute atoms is conserved during growth. Since they are not required to diffuse during transformation, the interfacial mobility is expected to be high even at low temperatures.

A semi-coherent interface containing a single array of anticoherency dislocations is considered to be glissile when the dislocations are able to move conservatively as the interface migrates. The dislocations must therefore all be pure screw dislocations, or have Burger's vectors which do not lie in the interface plane. The interface plane is the irrational invariant-plane or habit plane of the bainite plate. A glissile interface also requires that the glide planes (of the anticoherency dislocations) associated with the ferrite lattice must meet the corresponding glide planes in the austenite lattice edge to edge in the interface along the dislocation lines (Christian and Crocker, 1980).

If more than one set of anticoherency dislocations exist, then these should either have the same line vector in the interface, or their respective Burger's vectors must be parallel (Christian and Crocker, 1980). This condition ensures that the interface can move as an integral unit. It also implies that the deformation caused by the anticoherency dislocations, when the interface moves can always be described as a simple shear (caused by a resultant anticoherency dislocation which is a combination of all the anticoherency dislocations) on some plane which makes a finite angle with the interface plane, and intersects the latter along the line vector of the resultant anticoherency dislocation.

Obviously, if the anticoherency dislocation structure consists of just a single set of parallel dislocations, or of a set of different dislocations which can be summed to give a single glissile anticoherency dislocation, then it follows that there must exist in the interface, a line which is parallel to the resultant anticoherency dislocation line vector, along which there is zero distortion. Because this line exists in the interface, it is also unrotated. It is an *invariant-line* in the interface between the parent and product lattices. When full coherency is not possible between the two structures (as is the case for the FCC to BCC transformation), then for the interface to be glissile, the transformation strain relating the two lattices must be an invariant-line strain, with the invariant-line lying in the interface plane.

An interesting consequence of the restriction that the transformation strain must be an invariant-line strain is that models of the ferrite–austenite interface as a single array of anticoherency dislocations are not possible for any orientation between Nishiyama–Wasserman and Kurdjumov–Sachs if the most densely-packed planes of the two structures are regarded as exactly parallel (Knowles and Smith, 1982; Christian, 1990a). This is because for realistic values of the lattice parameters, it is not possible to obtain a transformation strain which is an invariant-line strain if the planes are exactly parallel. If it is assumed that the interface contains just one set of anticoherency dislocations then the predicted orientation relation always has the most densely-packed planes of the two structures at a small angle (about 0.5°) to each other – such a small deviation is unfortunately difficult to detect experimentally.

There have been a few recent high resolution studies of the interface between bainite and austenite (e.g. Kajiwara *et al.*, 1999). It has not, however, been recognised that it is necessary to characterise the strain fields of any defects in the interface in order to make deductions about the mechanism of transformation. False conclusions can be reached about atomic steps if work is not done to reveal whether these are pure steps or coherency dislocations whose motion accomplishes transformation.

2.5.6 The Crystallography of a Lath of Bainite

The sub-units of a bainite sheaf may adopt the morphology of a plate or of a lath, where the latter is idealised as a parallelepiped of dimensions a, b, and c, with $a > b > c$. The lath shape is adopted when the transformation occurs at high temperatures. The crystallography of such laths has been characterised in detail and to a high level of accuracy, by Davenport (1974), as follows:

Growth direction	$[\bar{1}\,0\,1]_\gamma \| [\bar{1}\,\bar{1}\,1]_\alpha$
Habit plane (area $= ab$)	$(2\,3\,2)_\gamma \simeq (\bar{1}\,5\,4)_\alpha$
Face of area $= ac$	$(1\,0\,1)_\gamma$
Orientation relationship (KS)	$[\bar{1}\,0\,1]_\gamma \| [\bar{1}\,\bar{1}\,1]_\alpha$ $(111)_\gamma \| (011)_\alpha$

when the crystallography is, for consistency, stated in the standard variant described earlier. Hence, the major growth direction of each lath corresponds to the parallel close-packed directions from the α and γ lattices. This is consistent with less direct trace analysis results which indicated that the major growth direction of the laths lies along $< \bar{1}\,\bar{1}\,1 >_\alpha$ (Goodenow and Hehemann, 1965; Oblak and Hehemann, 1967; Ohmori and Honeycombe, 1971). The habit plane indices are significantly different from earlier data which indicated a $\{1\,1\,1\}_\gamma$ habit (Greninger and Troiano, 1940; Oblak and Hehemann, 1967; Ohmori, 1971b; Ohmori and Honeycombe, 1971) but those analysis were either of insufficient precision or were concerned with the apparent habit planes of sheaves (Davenport, 1974). Davenport also demonstrated that sets of two groups of laths with a common growth direction, but with virtually orthogonal habit planes, tended to form in close proximity. There is as yet, no detailed analysis available which can predict these results.

Sandvik (1982a) has measured, using single surface trace analysis, the habit planes of individual sub-units. The mean habit plane is close to $(0.373\ 0.663\ 0.649)_\gamma$ for an orientation relationship in which $(1\,1\,1)_\gamma \| (0\,1\,1)_\alpha$ and $[\bar{1}\,0\,1]_\gamma$ is approximately 4° from $[\bar{1}\,\bar{1}\,1]_\alpha$ (such an orientation is close to the Nishiyama–Wasserman orientation relationship). The habit plane was not found to vary significantly with transformation temperature. Using data from high-resolution observations of the displacements of austenite twins by the shape deformation due to transformation, he was able to show that the shear component of the shape strain of a sub-unit is about 0.22. Sandvik also showed that the observed shape strain direction and magnitude are close to the corresponding parameters for the classic $\{2\,2\,5\}_\gamma$ and $\{3\,10\,15\}_\gamma$ martensites in steels.

2.5 Microstructure of Bainite: The Midrib

High-carbon steels can sometimes transform to plates of lower bainite which do not have a homogeneous microstructure (Okamoto and Oka, 1986). When observed using light microscopy, a macroscopic plate of lower bainite is seen to have a black line running centrally along its axis (Fig. 2.26). Transmission electron microscopy reveals that this line corresponds to a centrally located, coplanar thin plate of martensite which is sandwiched between regions of lower bainite. The lower bainite containing the midrib is actually found to

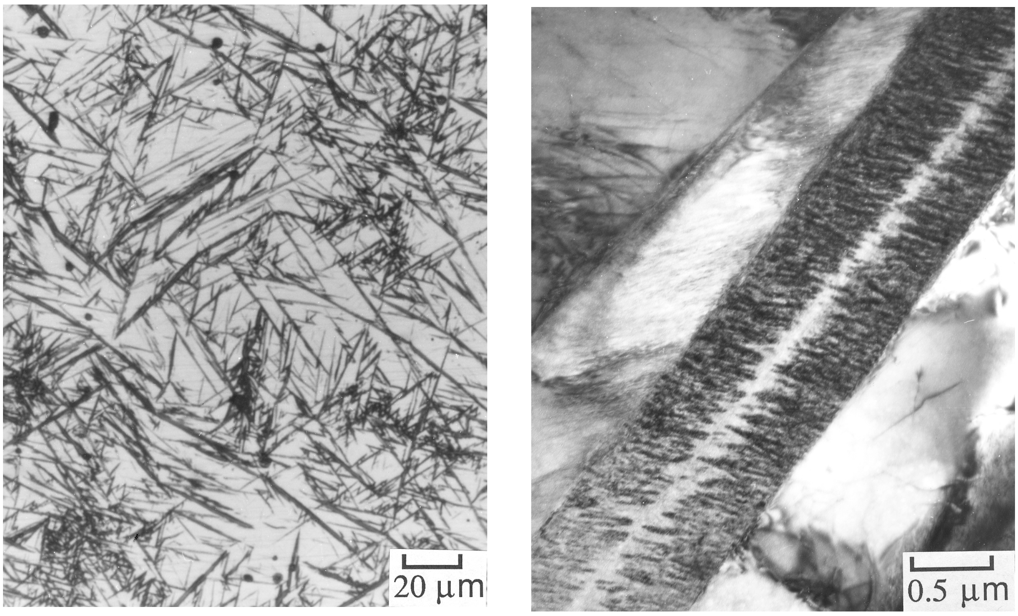

Fig. 2.26 Optical and transmission electron micrographs of the midrib associated with lower bainite in a plain carbon steel (after Okamoto and Oka, 1986).

evolve in two stages, from thin-plate martensite which forms first by the isothermal transformation of austenite, and which then stimulates the growth of the adjacent bainite regions.

Okamoto and Oka deduced that at relatively high transformation temperatures, the steels react to give lower bainite without a midrib, but as the transformation temperature is reduced to below a certain temperature T_r, this is replaced by the lower bainite with a thin-plate martensite midrib, which then gives way to just the thin-plate martensite; at a sufficiently low temperature (below the conventional M_S temperature), ordinary martensite with a lenticular plate morphology forms by the athermal transformation of austenite.

It was noted above that both the lower bainite containing the midrib, and thin-plate martensite isothermally form in the temperature range $T_r \rightarrow M_S$. Okamoto and Oka demonstrated that the difference between these two temperatures diminishes as the carbon concentration of the steel decreases, until at about 1wt% C, it becomes zero. Consequently, neither of these phases have been reported to occur in lower carbon steels.

The terminology *thin-plate martensite* has its origins in work done on nickel-rich Fe–Ni–C alloys, where the martensite transformation temperatures are well below -100°C (Maki *et al.*, 1973, 1975). The martensite then tends to form as extremely thin, parallel-sided plates in preference to much thicker lenticular plates, especially as the carbon concentration is increased. Because of their large aspect ratios, the thin plates are elastically accommodated in the austenite matrix; their interfaces remain glissile. The plates can therefore thicken as the temperature is reduced, or indeed become thinner as the temperature is raised.

2.7 Summary

Bainite grows in the form of clusters of thin lenticular plates or laths, known as sheaves. The plates within a sheaf are known as sub-units. The growth of each sub-unit is accompanied by an invariant-plane strain shape change with a large shear component. The sub-units are to some extent separated from each other by films of residual phases such as austenite or cementite, so that the shape strain of the sheaf as a whole tends to be much smaller than that of an isolated sub-unit. The plates within any given sheaf tend to adopt almost the same crystallographic orientation and have identical shape deformations. Because of the relatively high temperatures at which bainite grows (where the yield stresses of ferrite and austenite are reduced), the shape strain causes plastic deformation which in turn leads to a relatively large dislocation density in both the parent and product phases; other kinds of defects, such as twinning and faulting are also found in the residual austenite. This plastic accommodation of the shape change explains why each sub-unit grows to a limited size which may be far less than the austenite grain size. The dislocation debris stifles the motion of the otherwise glissile interface. Consequently, the sheaf as a whole grows by the repeated 'nucleation' of new sub-units, mostly near the tips of those already existing.

The bainitic ferrite/austenite orientation relationship is always found to lie well within the Bain region; this and other features of the transformation are broadly consistent with the phenomenological theory of martensite crystallography. The growth of bainitic ferrite undoubtedly occurs without any redistribution of iron or substitutional solute atoms, even on the finest conceivable scale at the transformation interface. Although some excess carbon is retained in solution in the bainitic ferrite after transformation, most of it is partitioned into the residual austenite, and in the case of lower bainite, also precipitated as carbides within the ferrite. This redistribution of carbon could of course occur after the diffusionless growth of bainitic ferrite, and the subject is discussed in more detail in Chapters 5 and 6. All of the observed characteristics of bainitic ferrite prove that it grows by a displacive transformation mechanism.